

Tracing Magnetic Fields with Ground State Alignment

Huirong Yan^a, and A. Lazarian^b

^a*Peking University, KIAA, 5 Yi He Yuan Rd, Beijing, 100871, China, e-mail: hryan@pku.edu.cn*

^b*University of Wisconsin-Madison, Astronomy Department, 475 N. Charter St., Madison, WI 53706, US, e-mail: lazarian@astro.wisc.edu*

Abstract

Observational studies of magnetic fields are vital as magnetic fields play a crucial role in various astrophysical processes, including star formation, accretion of matter, transport processes (e.g., transport of heat), and cosmic rays. The existing ways of magnetic field studies have their limitations. Therefore it is important to explore new effects which can bring information about magnetic field. We identified a process "ground state alignment" as a new way to determine the magnetic field direction in diffuse medium. The consequence of the process is the polarization of spectral lines resulting from scattering and absorption from aligned atomic/ionic species with fine or hyperfine structure. The alignment is due to anisotropic radiation impinging on the atom/ion, while the magnetic field induces precession and realign the atom/ion and therefore the polarization of the emitted or absorbed radiation reflects the direction of the magnetic field. The atoms get aligned at their low levels and, as the life-time of the atoms/ions we deal with is long, the alignment induced by anisotropic radiation is susceptible to extremely weak magnetic fields ($1\text{G} \gtrsim B \gtrsim 10^{-15}\text{G}$). Compared to the upper level Hanle effect, atomic realignment is most suitable for the studies of magnetic field in the diffuse medium, where magnetic field is relatively weak. The corresponding physics of alignment is based on solid foundations of quantum electrodynamics and in a different physical regime the alignment has become a part of solar spectroscopy. In fact, the effects of atomic/ionic alignment, including the realignment in magnetic field, were studied in the laboratory decades ago, mostly in relation to the maser research. Recently, the atomic effect has been already detected in observations from circumstellar medium and this is a harbinger of future extensive magnetic field studies. It is very encouraging that a variety of atoms with fine or hyperfine splitting of the ground or metastable states exhibit the alignment and the resulting polarization degree in some cases exceeds 20%. A unique feature of the atomic realignment is that they can reveal the 3D orientation of magnetic field. In this article, we shall review the basic physical processes involved in atomic realignment. We shall also discuss its applications to interplanetary, circumstellar and interstellar magnetic fields. In addition,

our research reveals that the polarization of the radiation arising from the transitions between fine and hyperfine states of the ground level can provide a unique diagnostics of magnetic fields, including those in the Early Universe.

Key words: ground state alignment (GSA), magnetic field, polarization, spectral lines,

1 Introduction

Astrophysical magnetic fields are ubiquitous and extremely important, especially in diffuse media, where their energy is comparable or exceeds the energy of thermal gas. For instance, in the diffuse interstellar medium (ISM), magnetic field pressure may exceed the thermal pressure by a factor of ten. In contrast, only a few techniques are available for the studies of magnetic field in diffuse medium and each of them has its own limitation. The Zeeman splitting can sample only relatively strong magnetic fields in dense and cold clouds (see [1]). In most cases, only the line-of-sight component of the field can be obtained. In some cases, the disentangling of the magnetic field and density fluctuations is nontrivial. For instance, the Faraday rotation is sensitive to the product of the electron density and the line-of-sight magnetic field (see [2]). Finally, all techniques have their area of applicability, e.g. polarization of the synchrotron emission traces the plane-of-sky magnetic fields of the galactic halo (see [3]). New promising statistical techniques can measure the *average* direction of magnetic field using spectral line fluctuations ([4], [5], [6]) or synchrotron intensity fluctuations [7].

The closest to the discussed technique of ground state alignment (henceforth GSA) are the techniques based on grain alignment and the Hanle effect. It is well known that the extinction and emission from aligned grains reveal magnetic field direction perpendicular to the line of sight (see [8] for a review). In spite of the progress in understanding of grain alignment (see [9] for a review), the natural variations in grain shapes and compositions introduce uncertainties in the expected degree of polarization. In contrast, Hanle measurements were proposed for studies of circumstellar magnetic fields and require much higher magnetic fields [10].

We should mention that all techniques suffer from the line-of-sight integration, which makes the tomography of magnetic fields difficult. As for the relative value, the most reliable is the Zeeman technique, but it is the technique that requires the strongest fields to study. In general, each technique is sensitive to magnetic fields in a particular environment and the synergetic use of the technique is most advantageous. Obviously, the addition of a new technique

is a very unique and valuable development.

Here we discuss a new promising technique to study magnetic fields in diffuse medium. As we discuss below, the physical foundations of these technique can be traced back to the laboratory work on atomic alignment in the middle of the previous century ([11]; [12]; [13]; [14]; [15]; see §2.2 for details). Later papers [16] and [17] considered isolated individual cases of application of the aligned atoms mostly within toy models (see below for a brief review of the earlier development). Yan & Lazarian (Yan and Lazarian [18], [19], [20], [21]) provided detailed calculations of GSA for a number of atoms and through their study identified GSA as a very unique new technique applicable for studying magnetic fields in a variety of environments, from circumstellar regions to the Early Universe. The emission and absorption lines ranging from radio to far UV were discussed. In particular, we identified new ways of study of magnetic fields using *absorption lines* (see [18]), radio lines arising from fine and hyperfine splitting [20] and provided extensive calculations of expected polarization degree for a variety of ions and atoms most promising to trace magnetic fields in diffuse interstellar gas, protoplanetary nebula etc.

The GSA technique as it stands now employs spectral-polarimetry and makes use of the ability of atoms and ions to be aligned *in their ground state* by the external anisotropic radiation. The aligned atoms interact with the astrophysical magnetic fields to get realigned.

It is important to notice that the requirement for the alignment in the ground state is the fine or hyperfine splitting of the ground state. The latter is true for many species present in diffuse astrophysical environments. Henceforth, we shall not distinguish atoms and ions and use word “atoms” dealing with both species. This technique can be used for interstellar¹, and intergalactic studies as well as for studies of magnetic fields in QSOs and other astrophysical objects.

We would like to stress that the effect of ground-state atomic alignment is based on the well known physics. In fact, it has been known that atoms can be aligned through interactions with the anisotropic flux of resonance emission (or optical pumping, see review [22] and references therein). Alignment is understood here in terms of orientation of the angular momentum vector \mathbf{J} , if we use the language of classical mechanics. In quantum terms this means a difference in the population of sublevels corresponding to projections of angular momentum to the quantization axis. There have been a lot of applications since the optical pumping was discovered by Kastler [11], ranging from atomic clocks, magnetometer, quantum optics and spin-polarized nuclei (see review by Budker and Romalis [23]; book by Cohen-Tannoudji et al. [15]). We will ar-

¹ Here interstellar is understood in a general sense, which, for instance, includes reflection nebulae.

gue in our review that similar fundamental changes GSA can induce in terms of understanding magnetic fields in diffuse media.

1.1 Earlier work on atomic alignment

It is worth mentioning that atomic realignment in the presence of magnetic field was also studied in laboratory in relation with early-day maser research (see [14]). Although our study in YL06 revealed that the mathematical treatment of the effect was not adequate in the original paper², the importance of this pioneering study should not be underestimated. The astrophysical application of the GSA was first discussed in the interstellar medium context by [24] for an atom with a hyperfine splitting. Varshalovich [16] pointed out that GSA can enable one to detect the direction of magnetic fields in the interstellar medium, and later in [25] they proposed alignment of Sodium as a diagnostics of magnetic field in comet's head though the classical approach they used to describe the alignment in the presence of magnetic field is incorrect.

Nearly 20 years after the work by Varshalovich, a case of emission of an idealized fine structure atom subject to a magnetic field and a beam of pumping radiation was conducted in [17]. However, in that case, a toy model of a process, namely, an idealized two-level atom was considered. In addition, polarization of emission from this atom was discussed for a very restricted geometry of observations, namely, the magnetic field is along the line of sight and both of these directions are perpendicular to the beam of incident light. This made it rather difficult to use this study as a tool for practical mapping of magnetic fields in various astrophysical environments.

The GSA we deal with in this review should not be confused with the Hanle effect that solar researcher have extensively studied. While both effects are based on similar atomic physics and therefore share some of the quantum electrodynamic machinery for their calculations, the domain of applicability of the effects is very different. In particular, Hanle effect is depolarization and rotation of the polarization vector of the resonance scattered lines in the presence of a magnetic field, which happens when the magnetic splitting becomes comparable to the decay rate of the excited state of an atom. The research into emission line polarimetry resulted in important change of the views on solar chromosphere (see [26], [27], [28], [29], [30], [31]). However, these studies correspond to a setting different from the one we consider in the case of GSA. The latter is the weak field regime, for which the Hanle effect is negligible. As we mentioned earlier, in the GSA regime the atoms/ions at ground level are

² Radiative pumping is much slower than magnetic mixing. Radiation was chosen as the quantization axis, nevertheless, which inevitably would lead to the nonzero coherence components. They were neglected in [14], however.

repopulated due to magnetic precession. While Hanle effect is prominent in the Solar case, it gets too weak for the environments of interstellar media, circumstellar regions and plasmas of Early Universe. These are the areas where the GSA effect is expected to be very important.

The realignment happens if during the lifetime of an atomic state more than one Larmor precession happens. The time scale of atomic precession scales as $0.011(5\mu G/B)$ s. As the life time of the ground state is long typically (determined by absorption rate, see table 1), even extremely weak magnetic fields can be detected this way. On the contrary, the typical application of the Hanle effect includes excited states with typical life-times of $A^{-1} \gtrsim 10^7$. Therefore, unlike GSA Hanle effect is used for studies of relatively strong magnetic fields, e.g. magnetic fields of the stars (see [32]).

Full calculations of alignment of atom and ions in their ground or metastable state in the presence of magnetic field were done in [18], [19], [20] considers polarization of absorbed light arising from aligned atoms with fine structure, [19] extends the treatment to emission and atoms with hyperfine, as well as, fine and hyperfine structure. [20] addresses the issues of radio emission arising from the transitions between the sublevels of the ground state and extended the discussions to the domain of both stronger and weaker magnetic field when the Hanle and ground level Hanle effects are present.

The polarization arising from GSA is on its way of becoming an accepted tool for interstellar and circumstellar studies. We see some advances in this direction. For instance, polarization of absorption lines arising from GSA was predicted in YL06 and was detected for the polarization of $H\alpha$ absorption in [33] though they neglected the important realignment effect of magnetic field in their analysis. Focused on atomic fluorescence, Nordsieck [34] discussed observational perspective using pilot spectroscopic observation of NGC as an example. We are sure that more detection of the predicted polarization will follow soon. Therefore we believe that the time is ripe to discuss the status of the GSA in the review in order to attract more attention of both observers and theorists to this promising effect.

In the review below we discuss three ways of using aligned atoms to trace magnetic field direction: 1) absorption lines 2) emission and fluorescent lines 3) emission and absorption lines related to transitions within splitting of the ground level

In addition, we shall discuss below how the information from the lines can be used to get the 3D structure of the magnetic fields, and, in particular cases, the intensity of magnetic field.

In terms of terminology, we will use "GSA" in the situations where magnetic field Larmor precession is important and therefore the alignment reveals

magnetic fields. Another possible term for the effect is "atomic magnetic re-alignment", which stresses the nature of the effect that we discuss. However, whenever this does not cause a confusion we prefer to use the term "GSA" in the analogy with the dust alignment which is in most cases caused by radiation and reveals magnetic field due to dust Larmor precession in external magnetic fields

In what follows, we describe in §2 the basic idea of GSA, then we give a brief review of experimental studies on optical pumping and atomic alignment. In §3, we expatiate on absorption polarimetry, which is an exclusive tracer of GSA, we discuss polarimetry of both fine and hyperfine transitions, how to obtain from them 3D magnetic field, different regimes of pumping, circular polarization. Emission polarimetry is presented in §4 and in §5, we discuss another window of opportunity in IR and submillimetre based on the fine structure transitions within the aligned ground state. In §6, the additional effect of GSA on abundance study is provided. In §7, we put GSA in a context of broad view of radiative alignment processes in Astrophysics. In §8, we focus on observational perspective and show a few synthetic observations with the input data on magnetic field from spacecraft measurements. Summary is provided in §9.

2 Basics of GSA

The basic idea of the GSA is very simple. The alignment is caused by the anisotropic deposition of angular momentum from photons of *unpolarized* radiation. In typical astrophysical situations the radiation flux is anisotropic³ (see Fig.1*right*). As the photon spin is along the direction of its propagation, we expect that atoms scattering the radiation from a light beam can be aligned. Such an alignment happens in terms of the projections of angular momentum to the direction of the incoming light. To study weak magnetic fields, one should use atoms that can be aligned in the ground state. For such atoms to be aligned, their ground state should have the non-zero angular momentum. Therefore fine (or hyperfine) structure is *necessary* for the alignment that we describe in the review.

Let us discuss a toy model that provides an intuitive insight into the physics of GSA. Consider an atom with its ground state corresponding to the total angular momentum $I = 1$ and the upper state corresponding to the angular momentum $I = 0$ [16] If the projection of the angular momentum to the

³ Modern theory of dust alignment, which is a very powerful way to study magnetic fields (see [9] and ref. therein) is also appealing to anisotropic radiation as the cause of alignment.

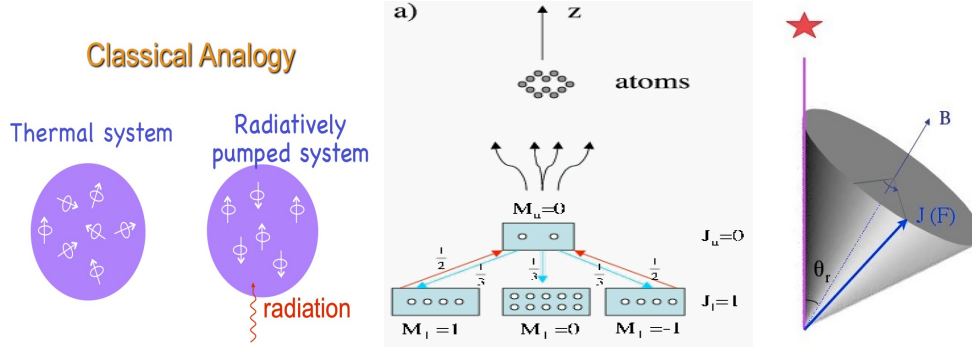


Fig. 1. *Upper left:* A cartoon illustrate classical analogy of the GSA induced by optical pumping; *Lower left:* A toy model to illustrate how atoms are aligned by anisotropic light. Atoms accumulate in the ground sublevel $M = 0$ as radiation removes atoms from the ground states $M = 1$ and $M = -1$; *Upper right:* Typical astrophysical environment where the ground-state atomic alignment can happen. A pumping source deposits angular momentum to atoms in the direction of radiation and causes differential occupations on their ground states. *Lower right:* In a magnetized medium where the Larmor precession rate ν_L is larger than the photon arrival rate τ_R^{-1} , however, atoms are realigned with respect to magnetic field. Atomic alignment is then determined by θ_r , the angle between the magnetic field and the pumping source. The polarization of scattered line also depends on the direction of line of sight, θ and θ_0 . (From [20])

direction of the incident resonance photon beam is M , the upper state M can have values $-1, 0$, and 1 , while for the upper state $M=0$ (see Fig.1left). The unpolarized beam contains an equal number of left and right circularly polarized photons whose projections on the beam direction are 1 and -1 . Thus absorption of the photons will induce transitions from the $M = -1$ and $M = 1$ sublevels. However, the decay from the upper state populates all the three sublevels on ground state. As the result the atoms accumulate in the $M = 0$ ground sublevel from which no excitations are possible. Accordingly, the optical properties of the media (e.g. absorption) would change.

The above toy model can also exemplify the role of collisions and magnetic field. Without collisions one may expect that all atoms reside eventually at the sublevel of $M = 0$. Collisions, however, redistribute atoms to different sublevels. Nevertheless, as the randomization of the ground state requires spin flips, it is less efficient than one might naively imagine [14]. For instance, experimental study in [35] suggests that more than 10 collisions with electrons. are necessary to destroy the aligned state of sodium. The reduced sensitivity of aligned atoms to disorienting collisions makes the effect important for various astrophysical environments.

Owing to the precession, the atoms with different projections of angular momentum will be mixed up. Magnetic mixing happens if the angular momentum precession rate is higher than the rate of the excitation from the ground

state, which is true for many astrophysical conditions, e.g., interplanetary medium, ISM, intergalactic medium, etc. As a result, angular momentum is redistributed among the atoms, and the alignment is altered according to the angle between the magnetic field and radiation field θ_r (see Fig.1*right*). This is the *classical* picture.

In *quantum* picture, if magnetic precession is dominant, then the natural quantization axis will be the magnetic field, which in general is different from the symmetry axis of the radiation. The radiative pumping is to be seen coming from different directions according to the angle between the magnetic field and radiation field θ_r , which results in different alignment.

The classical theory can give a qualitative interpretation which shall be utilized in this paper to provide an intuitive picture. Particularly for emission lines, both atoms and the radiation have to be described by the density matrices in order to obtain quantitative results. This is because there is coherence among different magnetic sublevels on the upper state⁴.

Our simple considerations above indicate that, in order to be aligned, first, atoms should have enough degrees of freedom: namely, the quantum angular momentum number must be ≥ 1 . Second, the incident flux must be anisotropic. Moreover, the collisional rate should not be too high. While the latter requires special laboratory conditions, it is applicable to many astrophysical environments such as the outer layers of stellar atmospheres, the interplanetary, interstellar, and intergalactic medium.

2.1 Relevant Timescales

Various species with fine structure can be aligned. A number of selected transitions that can be used for studies of magnetic fields are listed in [18, 19, 20] and table 3. Why and how are these lines chosen? We gathered all of the prominent interstellar and intergalactic lines ([36], [37]), from which we take only alignable lines, namely, lines with ground angular momentum number $J_g(or F_g) \geq 1$. The number of prospective transitions increases considerably if we add QSO lines. In fact, many of the species listed in the Table 1 in [38] are alignable and observable from the ground because of the cosmological redshifts.

In terms of practical magnetic field studies, the variety of available species

⁴ In quantum physics, quantum coherence means that subatomic particles are able to cooperate. These subatomic waves or particles not only know about each other, but are also highly interlinked by bands of shared electromagnetic fields so that they can communicate with each other.

$\nu_L(\text{s}^{-1})$	Larmor precession frequency	$\frac{eB}{m_e c}$	$88(B/5\mu\text{ G})$
$\tau_R^{-1}(\text{s}^{-1})$	radiative pumping rate	$B_{J_l J_u} I$	$7.4 \times 10^5 \left(\frac{R_*}{r}\right)^2$
$\tau_T^{-1}(\text{s}^{-1})$	emission rate within ground state	A_m	2.3×10^{-6}
$\tau_c^{-1}(\text{s}^{-1})$	collisional transition rate	$\max(f_{kj}, f_{sf})$	$6.4 \left(\frac{n_e}{0.1\text{cm}^{-3}} \sqrt{\frac{8000\text{K}}{T}}\right) \times 10^{-9}$

Table 1

Relevant rates for GSA. A_m is the magnetic dipole emission rate for transitions among J levels of the ground state of an atom. f_{kj} is the inelastic collisional transition rates within ground state due to collisions with electrons or hydrogens, and f_{sp} is the spin flip rate due to Van der Waals collisions. In the last row, example values for C II are given. τ_R^{-1} is calculated for an O type star, where R_* is the radius of the star radius and r is the distance to the star. (From [18])

is important in many aspects. One of them is a possibility of getting additional information about environments. Let us illustrate this by considering the various rates (see Table 1) involved. Those are 1) the rate of the Larmor precession, ν_L , 2) the rate of the optical pumping, τ_R^{-1} , 3) the rate of collisional randomization, τ_c^{-1} , 4) the rate of the transition within ground state, τ_T^{-1} . In many cases $\nu_L > \tau_R^{-1} > \tau_c^{-1}, \tau_T^{-1}$. Other relations are possible, however. If $\tau_T^{-1} > \tau_R^{-1}$, the transitions within the sublevels of ground state need to be taken into account and relative distribution among them will be modified (see YL06,c). Since emission is spherically symmetric, the angular momentum in the atomic system is preserved and thus alignment persists in this case. In the case $\nu_L < \tau_R^{-1}$, the magnetic field does not affect the atomic occupations and atoms are aligned with respect to the direction of radiation. From the expressions in Table 1, we see, for instance, that magnetic field can realign CII only at a distance $r \gtrsim 7.7\text{Au}$ from an O star if the magnetic field strength $\sim 5\mu\text{G}$.

If the Larmor precession rate ν_L is comparable to any of the other rates, the atomic line polarization becomes sensitive to the strength of the magnetic field. In these situations, it is possible to get information about the *magnitude* of magnetic field.

Fig.2 illustrates the regime of magnetic field strength where atomic realignment applies. Atoms are aligned by the anisotropic radiation at a rate of τ_R^{-1} . Magnetic precession will realign the atoms in their ground state if the Larmor precession rate $\nu_L > \tau_R^{-1}$. In contrast, if the magnetic field gets stronger so that Larmor frequency becomes comparable to the line-width of the upper level, the upper level occupation, especially coherence is modified directly by magnetic field, this is the domain of Hanle effect, which has been extensively discussed for studies of solar magnetic field (see [10] and references therein). When the magnetic splitting becomes comparable to the Doppler line width ν_D , polarization appears, this is the ‘‘magnetograph regime’’ [26]. For magnetic splitting $\nu_L \gg \nu_D$, the energy separation is enough to be resolved, and

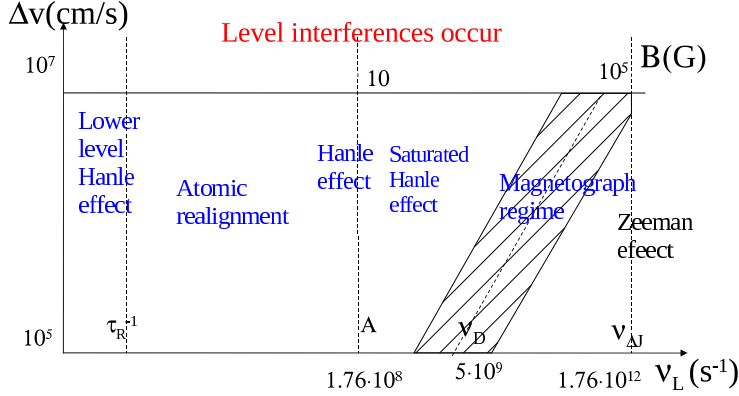


Fig. 2. Different regimes divided according to the strength of magnetic field and the Doppler line width. Atomic realignment is applicable to weak field ($< 1G$) in diffuse medium. Level interferences are negligible unless the medium is substantially turbulent ($\delta v \gtrsim 100\text{km/s}$) and the corresponding Doppler line width becomes comparable to the fine level splitting $\nu_{\Delta J}$. For strong magnetic field, Zeeman effect dominates. When magnetic splitting becomes comparable to the Doppler width, σ and π components (note: we remind the reader that σ is the circular polarization and π represents the linear polarization.) can still distinguish themselves through polarization, this is the magnetograph regime; Hanle effect is dominant if Larmor period is comparable to the lifetime of excited level $\nu_L^{-1} \sim A^{-1}$; similarly, for ground Hanle effect, it requires Larmor splitting to be of the order of photon pumping rate; for weak magnetic field ($< 1G$) in diffuse medium, however, GSA is the main effect provided that $\nu_L = 17.6(B/\mu G)\text{s}^{-1} > \tau_R^{-1}$. (From [18])

the magnetic field can be deduced directly from line splitting in this case. If the medium is strongly turbulent with $\delta v \sim 100\text{km/s}$ (so that the Doppler line width is comparable to the level separations $\nu_D \sim \nu_{\Delta J}$), interferences occur among these levels and should be taken into account.

Long-lived alignable metastable states that are present for some atomic species between upper and lower states may act as proxies of ground states. Absorptions from these metastable levels can also be used as diagnostics for magnetic field therefore.

The variety of species that are subject to the ground state or metastable state alignment render the GSA technique with really unique capabilities. Different species are expected to be aligned when the conditions for their existence and their alignment are satisfied. This allows to study the 3D distribution of magnetic fields, rather than line-average magnetic fields, which are available

through most of the alternative techniques.

2.2 *Experimental studies*

Unlike grain alignment, atomic alignment has been an established physical phenomena which has solid physical foundations and been studied and supported by numerous experiments (see review by [22]). The GSA was first proposed by Kastler [11], who received Nobel prize in 1966 for pointing out that absorption and scattering of resonant radiation, which is termed *optical pumping*, can induce imbalance on the ground state. Soon after that, the GSA was observed in experiments ([12]; [13]).

In experiments, there are two effective ways to detect the optical pumping, transmission and monitoring and fluorescence monitoring. Accordingly, we can use absorption spectropolarimetry and emission spectropolarimetry to probe GSA in astrophysical environment. In laboratory, special efforts need to be made to minimize the suppression of alignment by collisions, particularly with the wall, including injecting buffer gases and coating the container wall. In astrophysical environment, we have apparent advantage with only inter-atomic collisions and much lower density than the ultra-high vacuum chambers on earth. There can be two pumping mechanisms, depopulation pumping and repopulation pumping. The mechanism illustrated in Fig.1 is depopulation mechanism, which only requires anisotropy of radiation. Repopulation pumping, on the other hand, occurs as a result of spontaneous decay of polarized excited state, which can only be achieved in the case of Hanle regime where magnetic field splitting is at least comparable to the natural line-width. For most diffuse medium in interstellar environment, the magnetic field is too weak to induce the Hanle effect.

There have been a lot of applications since the optical pumping was proposed as a way of ordering the spin degrees of freedom, ranging from clocks, magnetometer, quantum optics and spin-polarized nuclei. In contrast, the actual applications to astrophysics so far are only limited to Hanle effect in stellar atmosphere and masers ([39]; [40]; [41]; [42]). The magnetic diagnostics with the GSA has not gone far from theoretical predictions and it is our goal through this review to make the idea widely spread in the community.

We feel that the percolation of the ideas of optical pumping to different astrophysical areas resulted in substantial and sometimes revolutionary changes. For instance, when the solar community rediscovered this effect in their context this resulted in a series of high impact publications, new measurements, substantially better understanding of processes etc. (see [10]). The ideas of magnetic field studies using aligned atoms are at the transitional stage of get-

ting accepted by the astrophysical community. We expect big advances as the GSA becomes an accepted tool.

3 Polarized absorption lines

The use of absorption lines to study magnetic fields with aligned atoms was suggested in [18]. Below we briefly outline the main ideas of the proposed techniques.

When atomic species are aligned on their ground state, the corresponding absorption from the state will be polarized as a result of the differential absorption parallel and perpendicular to the direction of alignment. The general expression for finite optical depth would be

$$\begin{aligned} I &= (I_0 + Q_0)e^{-\tau(1+\eta_1/\eta_0)} + (I_0 - Q_0)e^{-\tau(1-\eta_1/\eta_0)}, \\ Q &= (I_0 + Q_0)e^{-\tau(1+\eta_1/\eta_0)} - (I_0 - Q_0)e^{-\tau(1-\eta_1/\eta_0)}, \\ U &= U_0e^{-\tau}, V = V_0e^{-\tau}, \end{aligned} \quad (1)$$

where I_0, Q_0, U_0 are the Stokes parameters of the background radiation, which can be from a weak background source or the pumping source itself. d refers to the thickness of medium. η_0, η_1, η_2 are the corresponding absorption coefficients. In the case of unpolarized background radiation and thin optical depth, the degree of linear polarization is given by

$$P = \frac{Q}{I} = \frac{e^{-(\eta_0+\eta_1)d} - e^{-(\eta_0-\eta_1)d}}{e^{-(\eta_0+\eta_1)d} + e^{-(\eta_0-\eta_1)d}} \approx -\tau \frac{\eta_1}{\eta_0} \quad (2)$$

The polarization in this case has a simple relation given by

$$\frac{P}{\tau} = \frac{Q}{I\eta_0 d} \simeq \frac{-\eta_1}{\eta_0} = \frac{1.5\sigma_0^2(J_l, \theta_r) \sin^2 \theta w_{J_l J_u}^2}{\sqrt{2} + \sigma_0^2(J_l, \theta_r)(1 - 1.5 \sin^2 \theta)w_{J_l J_u}^2}. \quad (3)$$

with the alignment parameter $\sigma_0^2 \equiv \frac{\rho_0^2}{\rho_0^2}$, the normalized dipole component of density matrix of ground state, which quantifies the degree of alignment. For instance, for a state of angular momentum 1, the definition of $\rho_0^2 = [\rho(1, 1) - 2\rho(1, 0) + \rho(1, -1)]$ (see App.A.1). The generic definition is given in App.A. The sign of it gives the direction of alignment. Since magnetic field is the quantization axis, a positive alignment parameter means that the alignment is parallel to the magnetic field and a negative sign means the alignment is perpendicular to the magnetic field. θ is the angle between the line of sight and

J	1			3/2			2		
J'	0	1	2	1/2	3/2	5/2	1	2	3
$w_{JJ'}^2$	1	-0.5	0.1	0.7071	-0.5657	0.1414	0.5916	-0.5916	0.1690
J	5/2			3			7/2		
J'	3/2	5/2	7/2	2	3	4	5/2	7/2	9/2
$w_{JJ'}^2$	0.5292	-0.6047	0.1890	0.4899	-0.6124	0.2041	0.4629	-0.6172	0.2160
J	4			9/2			5		
J'	3	4	5	7/2	9/2	11/2	4	5	6
$w_{JJ'}^2$	0.4432	-0.6205	0.2256	0.4282	-0.6228	0.2335	0.4163	-0.6245	0.2402

Table 2

Numerical values of $w_{JJ'}^2$. J is the J value of the initial level and J' is that of the final level.

magnetic field. $w_{J_l J_u}^2$ defined below, is a parameter determined by the atomic structure

$$w_{J_l J_u}^K \equiv \left\{ \begin{array}{ccc} 1 & 1 & K \\ J_l & J_l & J_u \end{array} \right\} / \left\{ \begin{array}{ccc} 1 & 1 & 0 \\ J_l & J_l & J_u \end{array} \right\}. \quad (4)$$

The values of $w_{JJ'}^2$ for different pairs of J, J' are listed in Table 2. We see that it totally depends on the sign of $w_{JJ'}^2$, whether the alignment and polarization are either parallel or orthogonal. Once we detect the direction of polarization of some absorption line, we immediately know the direction of alignment.

The alignment is either parallel or perpendicular to the direction of symmetry axis of pumping radiation in the absence of magnetic field. Real astrophysical fluid though is magnetized, and the Larmor precession period is usually larger than the radiative pumping rate unless it is very close to the radiation source as we pointed out earlier. In this case, realignment happens and atomic species can be aligned either parallel or perpendicular to the local magnetic field. The switch between the two cases is always at the Van Vleck angle $\theta_r = 54.7^\circ, 180^\circ - 54.7^\circ$, where θ_r is the angle between the magnetic field and radiation. This is because the dipole component of the density matrix ρ_0^2 is proportional to \bar{J}_0^2 , which changes from parallel to perpendicular to the magnetic field at Van Vleck angle (eq.8). As the result the polarization of the absorption line also changes according to Eq.(3). *This turnoff at the Van Vleck angle is a generic feature regardless of the specific atomic species as long as the background source is unpolarized and it is in the atomic realignment regime.* In practice, this means that once we detect any polarization in absorption line, we get immediate information of the direction of magnetic field in the plane of

Species	Ground state	excited state	Wavelength(\AA)	P_{max}
S II	$4S_{3/2}^o$	$4P_{1/2,3/2,5/2}$	1250-1260	12%($3/2 \rightarrow 1/2$)
Cr I	$a7S_3$	$7P_{2,3,4}^o$	3580-3606	5%($3 \rightarrow 2$)
C II	$2P_{1/2,3/2}^o$	$2S_{1/2}, 2P_{1/2,3/2}, 2D_{3/2,5/2}$	1036.3-1335.7	15%($3/2 \rightarrow 1/2$)
Si II			989.9-1533.4	7%($3/2 \rightarrow 1/2$)
O I	$3P_{2,1,0}$	$3S_1, 3D_{1,2,3}$	911-1302.2	29%($2 \rightarrow 2$)
S I		$3S_1, 3P_{0,1,2}^o, 3D_{1,2,3}$	1205-1826	22%($1 \rightarrow 0$)
C I			1115-1657	18%($1 \rightarrow 0$)
Si I	$3P_{0,1,2}$	$3P_{0,1,2}^o, 3D_{1,2,3}^o$	1695-2529	20%($2 \rightarrow 1$)
S III			1012-1202	24.5%($2 \rightarrow 1$)
		$z4G_{5/2}^o$	3384.74	-0.7%
TiIII	$a4F_{3/2}$	$z4F_{5/2}^o$	3230.13	-0.7%
		$z4F_{3/2}^o$	3242.93	2.9%
		$z4D_{3/2}^o$	3067.25	2.9%
		$z4D_{1/2}^o$	3073.88	7.3%

Table 3

Absorption lines of selected alignable atomic species and corresponding transitions. Note only lines above 912\AA are listed. Data are taken from the Atomic Line List <http://www.pa.uky.edu/~peter/atomic/> and the NIST Atomic Spectra Database. The last column gives the maximum polarizations and its corresponding transitions. For those species with multiple lower levels, the polarizations are calculated for shell star ($T_{eff} = 15,000\text{K}$) in the strong pumping regime; in the weak pumping regime, the maximum polarizations are 19% for OI transition ($2 \rightarrow 2$), and 9% for SI transition ($2 \rightarrow 2$).

sky within 90 degree degeneracy. If we have two measurable, then according to eq.(3) both θ_r, θ can be determined. With θ_r known, the 90 degree degeneracy in the pictorial plane can be removed and we can get 3D information of magnetic field.

Fig.3 shows the dependence of polarization of S II absorption on θ_r, θ , which is representative for all polarization of absorption lines. From these plots, a few general features can be identified. At $\theta = 90^\circ$, the observed polarization reaches a maximum for the same θ_r and alignment, which is also expected from Eq.(3). This shows that atoms are indeed realigned with respect to magnetic field so that the intensity difference is maximized parallel and perpendicular to the field (Fig.1 *right*). At $\theta = 0^\circ, 180^\circ$, the absorption polarization is zero according to Eq.(3). Physically this is because the precession around the magnetic field makes no difference in the x, y direction when the magnetic field is

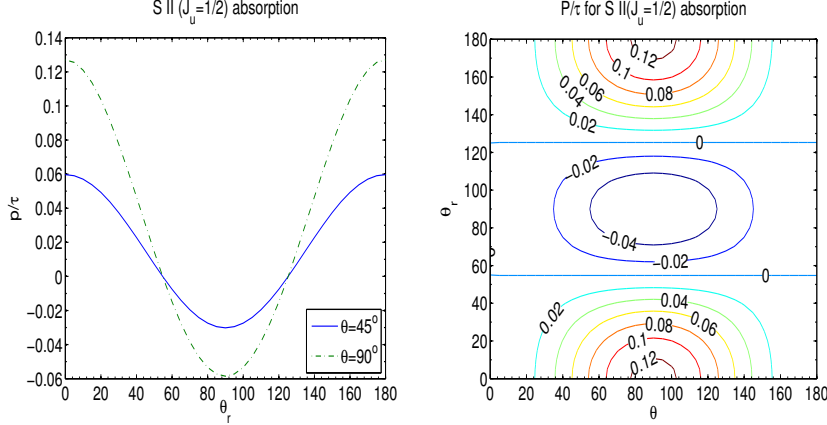


Fig. 3. *left*: Degree of polarization of S II absorption lines vs. θ_r , the angle between magnetic field and direction of pumping source θ , the angle between magnetic field and line of sight. *right*: The contour graphs of S II polarization. It is determined by the dipole component of density matrix $\sigma_0^2(\theta_r)$ and the direction of observation θ (Eq.3). From [18].

along the line of sight (Fig.1*right*).

We consider a general case where the pumping source does not coincide with the object whose absorption is measured. If the radiation that we measure is also the radiation that aligns the atoms, the direction of pumping source coincides with line of sight, *i.e.*, $\theta = \theta_r$ (Fig.1*right*).

3.1 Atoms with hyperfine structure

Although the energy of hyperfine interaction is negligible, the hyperfine interaction should be accounted for atoms with nuclear spins. This is because angular momentum instead of energy is the determinative factor. Hyperfine coupling increases the total angular momentum and the effects are two-sided. For species with fine structure ($J > 1/2$), the hyperfine interaction reduces the degree of alignment since in general the more complex the structure is, the less alignment is (see Fig.4). This is understandable. As polarized radiation is mostly from the sublevels with largest axial angular momentum, which constitutes less percentage in atoms with more sublevels. For species without fine structure ($J < 1/2$) like alkali, the hyperfine interaction enables alignment by inducing more sublevels⁵ (see [19]).

Note that the alignment mechanism of alkali is different from that illustrated in the carton (depopulation pumping) since the excitation rates from different

⁵ There are no energy splittings among them, the effect is only to provide more projections of angular momentum.

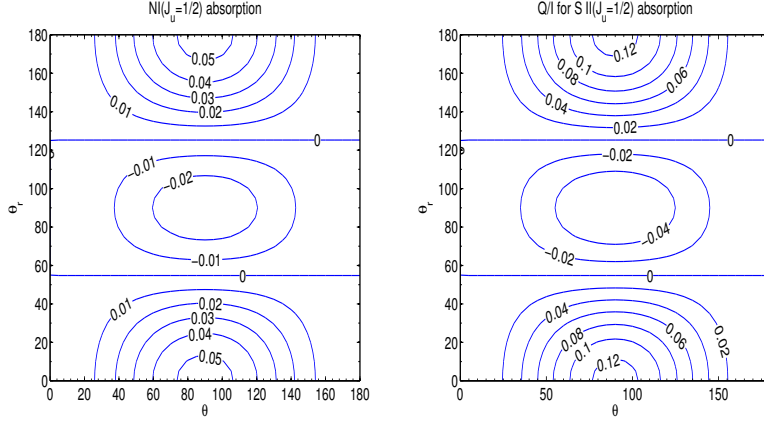


Fig. 4. *Left*: the schematics of N I hyperfine levels; and the contour graphs of N I (*middle*) and S II (*right*) degree of polarization. S II does not have nuclear spin. The degree of polarization is determined by the dipole component of density matrix $\sigma_0^2(\theta_r)$ and the direction of observation θ (Eq.3). N I and S II have the same electron configuration. However, N I has a nuclear spin while S II does not. More sublevels are allowed in the hyperfine structure of N I, and the alignment is thus reduced and so is the degrees of polarization of N I line compared to that of S II line. From [19].

sublevels on the ground state are equal. In other words, atoms from all the sublevels have equal probabilities to absorb photons. For the same reason, the absorption from alkali is not polarized⁶. The actual alignment is due to another mechanism, repopulation pumping. The alkali atoms are repopulated as a result of spontaneous decay from a polarized upper level (see [22]). Upper level becomes polarized because of differential absorption rates to the levels (given by $r_{kk'}$, see Eqs.10,12).

3.2 How to measure 3D magnetic field

Different from the case of emission, GSA is a unique mechanism to polarize absorption lines, which was first proposed by [18]. As illustrated above, 2D magnetic field in the plane of sky can be easily obtained by the direction of polarization. If we have quantitative measurement, we can get 3D magnetic field.

The resonance absorption lines in the Table 2 appropriate for studying magnetic fields in diffuse, low column density ($A_V \sim$ few tenths) neutral clouds in the interstellar medium are NI, OI, SII, MnII, and FeII. These are all in the ultraviolet.

At higher column densities, the above lines become optically thick, and lines of lower abundance, as well as excited states of the above lines become available.

⁶ Only if hyperfine structure can be resolved, polarization can occur.

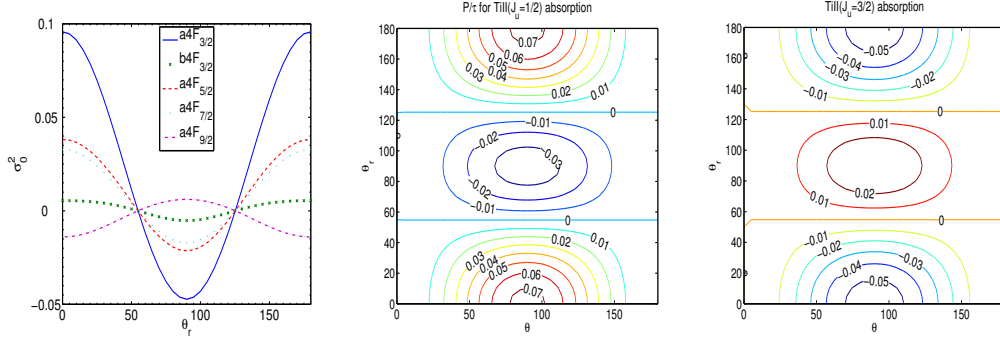


Fig. 5. *left*: the alignment of the ground state $a4F$ and metastable level $b4F_{3/2}$ of Ti II; *middle* and *right*: the contour of equal degree of polarization of Ti II absorption lines ($J_l = 1/2 \rightarrow J_u = 1/2, 3/2$). θ_r and θ are the angles of incident radiation and line of sight from the magnetic field (see Fig.2*right*). In the case of pumping source coincident with the background source, we have the degeneracy and polarization will be determined by one parameter $\theta_r = \theta$. From [20]

Significantly, some of these (TiII, FeI) are in the visible. An interesting region where the degenerate case (pumping along the line of sight) should hold is the "Orion Veil" [43], a neutral cloud with $A_V \sim 1.5$, and $N \sim 1000$, which is 1-2 parsec in the foreground of the Orion Nebula. The Orion Veil should be pumped by the Trapezium. This region is of particular interest for magnetic field studies, since it is one of the only places where maps exist of the HI 21 cm Zeeman Effect. This gives the sign and magnitude of the magnetic field along the line of sight. The magnetic realignment diagnostic, on the other hand, gives the orientation of the magnetic field lines in 3D, which is exactly complimentary information: combination of the two yields a complete 3D magnetic field map.

The TiII lines provide a fairly accessible test of the magnetic alignment diagnostic, although there are not enough strongly polarized lines in the visible to be useful by themselves: observation of an effect at TiII with moderate resolution would motivate a serious study of the pumping of the much more numerous FeI lines, and the construction of more advanced instrumentation. Table 3 shows the five strongest TiII lines, all from the $J = 3/2$ ground state of the ion (see also Fig.5). The polarization depends only on the J of the upper state, regardless of the other quantum numbers. We have assumed "weak pumping" for this calculation, so that the rate of decay from the excited states of the ground term exceeds the pumping rate. The most strongly polarized line, 3074, is unfortunately difficult from the ground, and the strongest line, 3384, is only weakly polarized. The 3243 line is the most favorable. It is estimated that for a line with $\tau \sim 1$ and a width of 20 km/sec, this effect would be detectable at 10σ for all stars brighter than $V=8$ with the spectropolarimeter at SALT with resolution $R = 6000$ (Nordsieck, private communications).

As a first step, with low resolution measurement, 2D magnetic field in the

pictorial plane can be easily obtained from the direction of polarization with a 90 degree degeneracy, similar to the case of grain alignment and Goldreich-Kylafis effect. Different from the case of emission, any polarization, if detected, in absorption lines, would be an exclusive indicator of alignment, and it traces magnetic field since no other mechanisms can induce polarization in absorption lines. The polarization in H α absorption that [33] reported in fact was due to the GSA as predicted in [18] for general absorptions.

If we have two measurable, we can solve Eq.3 and obtain θ_r , θ . With θ_r known, the 90 degree degeneracy can be removed since we can decide whether the polarization is parallel or perpendicular to the magnetic field in the plane of sky. Combined with θ , the angle between magnetic field and line of sight, we get 3D direction of magnetic field.

3.2.1 *Circumstellar Absorption*

The Be star ζ Tau illustrates one application of the diagnostic in circumstellar matter. A number of absorption lines from SiII metastable level $2P_{3/2}$ are seen, along with the OI and SII lines already discussed. This provides for a large number of different species. In this case the absorption is likely being formed in a disk atmosphere, absorbing light from the disk and pumped by light from the star. The net polarization signal is integrated across the disk, and depends just on the magnetic field geometry and the inclination of the disk. In this case, the inclination is known from continuum polarization studies to be 79° [44]. The FUSP sounding rocket should be sensitive to these effects: ζ Tau is one of the brightest UV sources in the sky.

A second interesting circumstellar matter case is for planetary disks around pre-main sequence stars. In this case, pumping conditions are similar to those for comets in the Solar System: pumping rates on the order of 0.1 – 1 Hz, and realignment for fields greater than 10 – 100 mGauss. Conditions here are apparently conducive to substantial populations in CNO metastable levels above the ground term: Roberge, et al (2002) find strong absorption in the FUV lines (1000 - 1500 Ang) of OI (1D) and NI and SII (2D), apparently due to dissociation of common ice molecules in these disks (these are also common in comet comae). Since these all have $J_l > 1$, they should be pumped, and realigned. This presents the exciting possibility of detecting the magnetic geometry in planetary disks and monitoring them with time. Since these are substantially fainter sources, this will require a satellite facility.

3.3 Different regimes of pumping

Most atoms have sublevels on the ground state, among which there are magnetic dipole transitions. Although its transition probability is very low, it can be comparable to the optical pumping rate in regions far from any radiation source. Depending on how far away the radiation source is, there can be two regimes divided by the boundary where the magnetic dipole radiation rate A_m is equal to the pumping rate τ_R^{-1} . Inside the boundary, the optical pumping rate is much larger than the M1 transition rate A_m so that we can ignore the magnetic dipole radiation as a first order approximation. Further out, the magnetic dipole emission is faster than optical pumping so that it can be assumed that most atoms reside in the lowest energy level of the ground state and alignment can only be accommodated on this level. The two regimes are demarcated at r_1 (see Fig.6 *left*), where r_1 is defined by

$$\tau_R^{-1} = B_{J_l J_u} I_{BB} (R_*/r_1)^2 = A_m, \quad (5)$$

and I_{BB}, R_* are the intensity and radius of the pumping source. For different radiation sources, the distance to the boundary differs. For an O type star, the distance would be ~ 0.1 pc for species like C II, Si II, while for a shell star ($T_{eff} = 15,000$ K), it is as close as to $\sim 0.003 - 0.01$ pc. For the species like, C II, Si II the lowest level is not alignable with $J_l = 1/2$, and thus the alignment is absent outside the radius r_1 , which ensures that observations constrain the magnetic field topology within this radius.

3.4 Is there any circular polarization?

Note that if the incident light is polarized in a different direction with alignment, *circular polarization* can arise due to de-phasing though it is a 2nd order effect. Consider a background source with a nonzero Stokes parameter U_0 shining upon atoms aligned in Q direction⁷. The polarization will be precessing around the direction of alignment and generate a V component representing a circular polarization

$$\frac{V}{I\tau} \simeq \frac{\kappa_Q U_0}{\eta_I I_0} = \frac{\psi_\nu \eta_Q U_0}{\xi_\nu \eta_I I_0} \quad (6)$$

⁷ To remind our readers, The Stokes parameters Q represents the linear polarization along \mathbf{e}_1 minus the linear polarization along \mathbf{e}_2 ; U refers to the polarization along $(\mathbf{e}_1 + \mathbf{e}_2)/\sqrt{2}$ minus the linear polarization along $(-\mathbf{e}_1 + \mathbf{e}_2)/\sqrt{2}$ (see Fig.1 *right*).

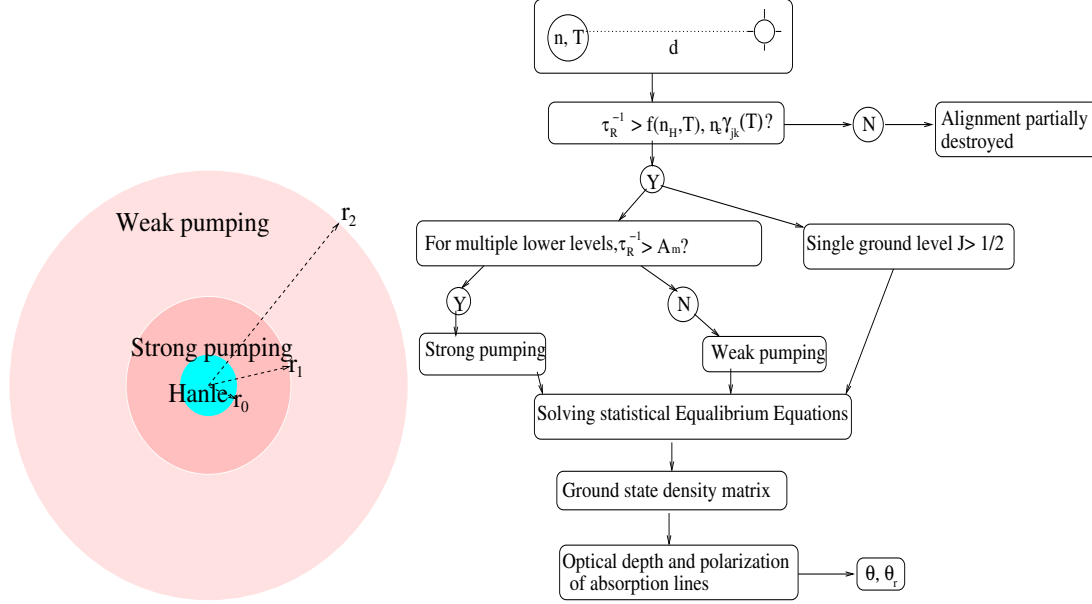


Fig. 6. *left*: a cartoon illustrating how the atomic pumping changes with distance around a radiation source. For circumstellar region, magnetic field is strong, such that the Hanle effect, which requires $\nu_L \sim A$, dominates. Atomic alignment applies to the much more distant interstellar medium, within r_2 , which is defined as the radius where the optical pumping rate τ_R^{-1} is higher than collisional rate. Inside r_2 , it can be further divided into two regimes: strong pumping and weak pumping, demarcated at r_1 (see Eq.5); *Right*: whether and how atoms are aligned depends on their intrinsic properties (transitional probabilities and structures) and the physical conditions: density n , temperature T and the averaged radiation intensity from the source I_* . If the pumping rate τ_R^{-1} is less than collisional rates, alignment is partially destroyed. Then for atoms with multiple lower levels, depending on the comparison between the pumping rate and the magnetic dipole radiation rate among the lower levels, the atoms are aligned differently. In the strong pumping case, all the alignable lower levels are aligned; on the contrary, only the ground level can be aligned in the case of weak pumping. From [18].

where κ is the dispersion coefficient, associated with the real part of the refractory index, whose imaginary part corresponds to the absorption coefficient η . ψ is the dispersion profile and ξ is the absorption profile.

The incident light can be polarized in the source, e.g. synchrotron emission from pulsars, or polarized through the propagation in the interstellar medium, e.g. as a result of selective extinction from the aligned dust grains (see [9]). In the latter case, the polarization of the impinging light is usually low and the intensity of circular polarization is expected to be low as well. This should not preclude the detection of the effect as the instrumentation improves.

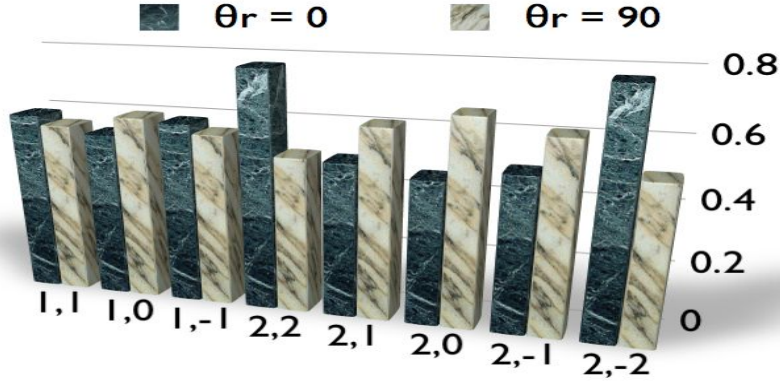


Fig. 7. The occupation in ground sublevels for Na. It is modulated by the angle between magnetic field and the radiation field θ_r .

4 Polarization of resonance and fluorescence lines

When the magnetic precession rate becomes less than the emission rate of the upper level, the effect of magnetic field on the upper level is negligible. The only influence of magnetic field is on the ground state through the alignment of atoms. This is the effect that was the focus of our studies in [18, 19, 20]. The atoms are aligned either parallel or perpendicular to the magnetic field as we discussed before.

The differential occupation on the ground state (see Fig.7) can be transferred to the upper level of an atom by excitation.

$$\rho_q^k(J_u) = \frac{1}{\sum_{J_l''} A'' + iA\Gamma'q} \sum_{J_l'k'} [J_l'] \left[\delta_{kk'} p_{k'}(J_u, J_l') B_{lu} \bar{J}_0^0 + \sum_{Qq'} r_{kk'}(J_u, J_l', Q, q') B_{lu} \bar{J}_Q^2 \right] \rho_{-q'}^{k'}(\bar{J}_l)$$

The radiation tensors are defined as

$$\begin{aligned} \bar{J}_0^0 &= I_*, \bar{J}_0^2 = \frac{W_a}{2\sqrt{2}W} (2 - 3 \sin^2 \theta_r) I_*, \bar{J}_{\pm 2}^2 = \frac{\sqrt{3}W_a}{4W} \sin^2 \theta_r I_* e^{\pm 2i\phi_r}, \\ \bar{J}_{\pm 1}^2 &= \mp \frac{\sqrt{3}W_a}{4W} \sin 2\theta_r I_* e^{\pm i\phi_r} \end{aligned} \quad (8)$$

The definition of the parameters $p_k, r_{kk'}$ for atoms of fine and hyperfine are respectively given below:

$$p_k(J_u, J_l) = (-1)^{J_u + J_l + 1} \begin{Bmatrix} J_l & J_l & k \\ J_u & J_u & 1 \end{Bmatrix}, \quad (9)$$

$$r_{kk'}(J_u, J_l, Q, q') = (3[k, k', 2])^{1/2} \begin{Bmatrix} 1 & J_u & J_l \\ 1 & J_u & J_l \\ 2 & k & k' \end{Bmatrix} \begin{pmatrix} k & k' & 2 \\ q & q' & Q \end{pmatrix} \quad (10)$$

for fine structure and

$$p_k = [F_l](-1)^{F_u+F_l+k+1} \begin{Bmatrix} F_l & F_l & k \\ F_u & F'_u & 1 \end{Bmatrix} [F_u, F'_u]^{1/2} \begin{Bmatrix} J_u & J_l & 1 \\ F_l & F_u & I \end{Bmatrix} \begin{Bmatrix} J_u & J_l & 1 \\ F_l & F'_u & I \end{Bmatrix} \quad (11)$$

$$r_{kk'} = (-1)^{k'+q'} (3[k, k', 2])^{1/2} [F_u, F'_u]^{1/2} [F'_l] \begin{pmatrix} k & k' & 2 \\ q & q' & Q \end{pmatrix} \begin{Bmatrix} 1 & F_u & F'_l \\ 1 & F'_u & F'_l \\ 2 & k & k' \end{Bmatrix} \begin{Bmatrix} J_u & J_l & 1 \\ F'_l & F_u & I \end{Bmatrix} \begin{Bmatrix} J_u & J_l & 1 \\ F'_l & F'_u & I \end{Bmatrix} \quad (12)$$

for hyperfine structure.

Emission from such a differentially populated state is polarized, the corresponding emission coefficients of the Stokes parameters are [27]:

$$\epsilon_i(\nu, \Omega) = \frac{h\nu_0}{4\pi} An(J_u, \theta_r) \Psi(\nu - \nu_0) \sum_{KQ} w_{J_u J_l}^K \sigma_Q^K(J_u, \theta_r) \mathcal{J}_Q^K(i, \Omega), \quad (13)$$

where $n(J_u) = n\sqrt{[J_u]}\rho_0^0(J_u)$ is the total population on level J_u . For transitions involving hyperfine structures,

$$\eta_i(\nu, \Omega) = \frac{h\nu_0}{4\pi} Bn\xi(\nu - \nu_0)[J_l] \sum_{KQF_l} [F_l]\sqrt{3}(-1)^{1-J_u+I+F_l} \begin{Bmatrix} J_l & J_l & K \\ F_l & F_l & I \end{Bmatrix} \begin{Bmatrix} 1 & 1 & K \\ J_l & J_l & J_u \end{Bmatrix} \rho_Q^K(F_l) \mathcal{J}_Q^K(i, \Omega), \quad (14)$$

The irreducible unit tensors for Stokes parameters I, Q, U are:

$$\begin{aligned}
\mathcal{J}_0^0(i, \Omega) &= \begin{pmatrix} 1 \\ 0 \\ 0 \end{pmatrix}, \quad \mathcal{J}_0^2(i, \Omega) = \frac{1}{\sqrt{2}} \begin{bmatrix} (1 - 1.5 \sin^2 \theta) \\ -3/2 \sin^2 \theta \\ 0 \end{bmatrix}, \quad \mathcal{J}_{\pm 1}^2(i, \Omega) = \sqrt{3} e^{\pm i\phi} \begin{bmatrix} \mp \sin 2\theta/4 \\ \mp \sin 2\theta/4 \\ \mp 2i \sin \theta/4 \end{bmatrix}, \\
\mathcal{J}_{\pm 2}^2(i, \Omega) &= \sqrt{3} e^{\pm 2i\phi} \left\{ \begin{array}{l} \sin^2 \theta/4 \\ -(1 + \cos^2 \theta)/4 \\ \mp 2i \cos \theta/4 \end{array} \right\}. \tag{15}
\end{aligned}$$

where the unit polarization vectors $\mathbf{e}_1, \mathbf{e}_2$ are chosen to be parallel and perpendicular to the magnetic field in the plane of sky. From equations(7,13), we see that emission line can be polarized without GSA. This corresponds the textbook description of polarization of scattered lines. It can be shown that if the dipole and other higher order components of the ground state density matrix ρ_q^2 are zeros, we recover the classical result in the optically thin case

$$\epsilon_2 = \epsilon_3 = 0, \quad P = \frac{\epsilon_1}{\epsilon_0} = \frac{3E_1 \sin^2 \alpha}{4 - E_1 + 3E_1 \cos^2 \alpha} \tag{16}$$

where α is the scattering angle⁸. The polarizability is actually given by

$$E_1 = \frac{w_{J_u J_l}^2 r_{20}}{p_0} \tag{17}$$

for transitions in fine structure. If we account for the alignment by radiation, but ignore magnetic field, *ie.*, $\theta_r = 0$, then

$$E_1 = \frac{w_{J_u J_l}^2 [r_{20} + r_{22} \sigma_0^2(J_l) + \sqrt{2} p_2 \sigma_0^2(J_l)]}{\sqrt{2} p_0 + r_{02} \sigma_0^2} \tag{18}$$

For optically thin case, the linear polarization degree $p = \sqrt{Q^2 + U^2}/I = \sqrt{\epsilon_2^2 + \epsilon_1^2}/\epsilon_0$, the positional angle $\chi = \frac{1}{2} \tan^{-1}(U/Q) = \frac{1}{2} \tan^{-1}(\epsilon_2/\epsilon_1)$.

Since the weak magnetic field does not have direct influence on the upper level, there is no simple geometrical correspondence between the polarization and magnetic field as in the case of absorption. In fact, from the discussions above (eq.16), we see that polarization is either parallel or perpendicular to the radiation field in the absence of GSA. The effect of GSA is to introduce coherence on the upper level through the radiative excitation, which is then

⁸ Since there is no alignment on the ground state and we can choose the direction of radiation as the quantization axis, $\alpha = \theta$.

Species	Lower state	Upper state	Wavelength(\AA)	$ P_{max} $
S II	$4S_{3/2}^o$	$4P_{3/2}$	1253.81	30.6%
		$4P_{5/2}$	1259.52	31.4%
O I	$3P_0$	$3S^o$	1306	16%
		$3S^o$	1304	8.5%
	$3P_2$	$3S^o$	1302	1.7%
	$3P$	$3S^o$	5555,6046,7254	2.3%
	$3P_0$	$3D^o$	1028	4.29%
	$3P_1$	$3D^o$	1027	7.7%
	$3P_2$	$3D^o$	1025	10.6%
H I	$1S_{1/2}$	$2P_{3/2}$	912-1216	26%
		$2P_{3/2}$	5891.6	20%
Na I	$1S_{1/2}$	$2P_{3/2}$	7667,4045.3	21%
K I	$1S_{1/2}$	$2P_{3/2}$	1238.8	22%
N V	$1S_{1/2}$	$2P_{3/2}$	1117.977	27%
P V	$1S_{1/2}$	$2P_{3/2}$	1200	5.5%
N I	$4S_{3/2}^o$	$4P_{1/2}$	8643 \AA	20%
Al II	$1S_0$	$1P_1^o$		

Table 4

The maximum polarizations expected for a few example of emission lines and their corresponding transitions

transferred to emission. To obtain the direction of magnetic field, one needs quantitative measurements of at least two lines. The lines for which we have calculated the polarizations are listed in Table4.

In the case that the direction of optical pumping is known, e.g., in planetary system and circumstellar regions, magnetic realignment can be identified if the polarization is neither perpendicular or parallel to the incident radiation (see eqs.16,18). As an example, we show here polarization map from a spherical system with poloidal magnetic field [21], eg., a circumstellar envelope, the polarization is supposed to be spherically symmetric without accounting for the effect of the magnetic field. With magnetic realignment though, the pattern of the polarization map is totally different, see fig.8. *In practice, one can remove the uncertainty by measuring polarization from both alignable and non-alignable species, which does not trace the magnetic field.*

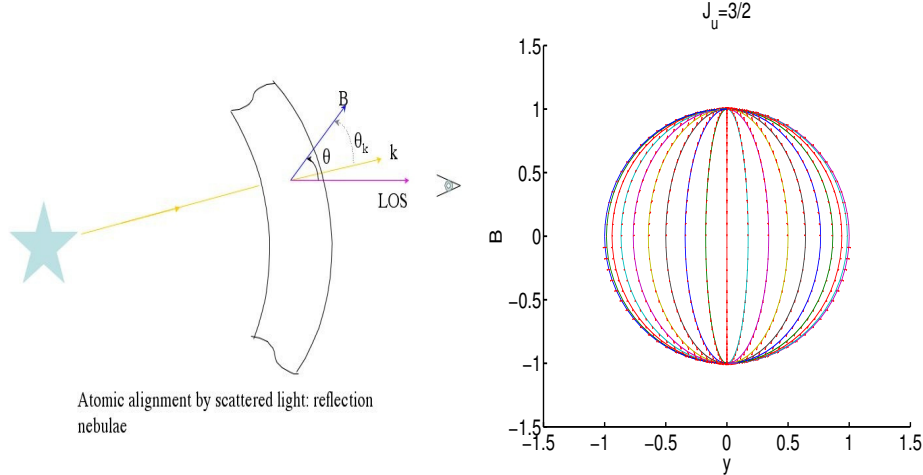


Fig. 8. *left*: schematics of GSA by by circumstellar scattering; *right*: Polarization vectors of OI emission in a circumstellar region with alignment by uniform magnetic field. The inclination of magnetic field is 45 degree from the light of sight. The magnetic field is in the y direction in the plane of sky (from [21]).

4.1 Fluorescence from reflection nebulae

The magnetic realignment diagnostic can also be used in fluorescent scattering lines. This is because the alignment of the ground state is partially transferred to the upper state in the absorption process. There are a number of fluorescent lines in emission nebulae that are potential candidates (see [34]). Although such lines have been seen in the visible in HII regions ([45, 46]) and planetary nebulae [47], we suggest that reflection nebulae would be a better place to test the diagnostic, since the lack of ionizing flux limits the number of levels being pumped, and especially since common fluorescent ions like NI and OI would not be ionized, eliminating confusing recombination radiation. Realignment should make itself evident in a line polarization whose position angle is not perpendicular to the direction to the central star. This deviation depends on the magnetic geometry and the scattering angle. The degree of polarization also depends on these two things. It will be necessary to compare the polarization of several species with different dependence on these factors to separate the effects. This situation is an excellent motivation for a pilot observation project.

5 IR/submillimetre transitions within ground state

The alignment on the ground state affects not only the optical (or UV) transitions to the excited state, but also the magnetic dipole transitions within the ground state. Similar to HI, other species that has a structure within

the ground state is also influenced by the optical pumping⁹ through the Wouthuysen-Field effect ([48],[49]). After absorption of a Ly α , the hydrogen atom can relax to either of the two hyperfine levels of the ground state, which can induce a HI 21cm emission if the atom falls onto the ground triplet state (see also [50] for a review). Recently, the oxygen pumping has been proposed as a probe for the intergalactic metals at the epoch of reionization [51].

However, in all these studies, the pumping light is assumed to be isotropic. This is problematic, particularly for the metal lines whose optical depth is small. During the early epoch of reionization, for instance, the ionization sources are localized, which can introduce substantial anisotropy. The GSA introduced by the anisotropy of the radiation field can play an important role in many circumstances. The earlier oversimplified approach can lead to a substantial error to the predictions. The emissivity and absorption coefficients for the Stokes parameters are modified due to the alignment effect. The ratio of corresponding optical depth to that without alignment is

$$\tilde{\tau} = \frac{\tau}{\tau_0} = \frac{\tilde{\eta} - \tilde{\eta}_{s,i} \exp(-T_*/T_s)}{1 - \exp(-T_*/T_s)}, \quad (19)$$

where T_* is the equivalent temperature of the energy separation of the metastable and ground level, T_s is the spin temperature.

$$\tilde{\eta}_i = \eta_1/\eta_1^0 = 1 + w_{0l}\sigma_0^2(J_l^0)\mathcal{J}_0^2(i, \Omega), \quad (20)$$

$$\tilde{\eta}_{s,i} = \tilde{\epsilon}_i = \epsilon_i/\epsilon_i^0 = 1 + w_{l0}\sigma_0^2(J_l)\mathcal{J}_0^2(i, \Omega) \quad (21)$$

are the ratios of absorption and stimulated emission coefficients with and without alignment, where $\mathcal{J}_0^2(i, \Omega)$ is given by Eq.(15). Since both the upper (metastable) level and the lower level are long lived and can be realigned by the weak magnetic field in diffuse medium, the polarization of *both emission and absorption* between them is polarized either parallel or perpendicular to the magnetic field like the case of all the absorptions from the ground state, and can be described by Eq.(3). In the case of emission, the dipole component of the density matrix in Eq.(3) should be replaced by that of the metastable level. In fig.9, we show an example of our calculation of the polarization of [C I] 610 μ m, which can be detected in places like PDRs.

We discussed pumping of hyperfine lines [H I] 21 cm and [N V] 70.7 mm in [19] and fine line [O I] 63.2 μ m here. Certainly this effect widely exists in all atoms with some structure on ground state, e.g., Na I, K I, fine structure lines, [C I], [C II], [Si II], [N II], [N III], [O II], [O III],[S II], [S III], [S IV], [Fe II],

⁹ To clarify, we do not distinguish between pumping by optical lines or UV lines, and name them simply "optical pumping".

Lines	Lower level	Upper level	Wavelength (μm)	P_{max}
[CI]	$3P_0$	$3P_1$	610	20%
[OI]	$3P_2$	$3P_1$	63.2	24%
[CII]	$3P_{1/2}$	$3P_{3/2}$	157.7	2.7%
[SiII]	$3P_{1/2}$	$3P_{3/2}$	34.8	4%
[SIV]	$3P_{1/2}$	$3P_{3/2}$	610	10.5%

Table 5

The polarization of forbidden lines.

etc (see Table 4.1 in [52]). The example lines we have calculated are listed in Table 5. Many atomic radio lines are affected in the same way and they can be utilized to study the physical conditions, especially in the early universe: abundances, the extent of reionization through the anisotropy (or localization) of the optical pumping sources, and *magnetic fields*, etc.

5.1 Magnetic field in PDR regions

Most fine structure FIR lines arise from photon dominated (PDR) region, a transition region between fully ionized and molecular clouds illuminated by a stellar source of UV radiation. The line ratio of the brightest ones, e.g., [C II] $158\mu m$, [O I] $63, 145\mu m$, are used to infer physical parameters, including density and UV intensity based on the assumption that they are collisionally populated. Recent observations of UV absorption by Sterling et al. [53], however, find that the population ratio of $3P_{1,0}$, the originating levels of [O I] $63, 145\mu m$ is about twice the LTE value in the planetary nebula (PN) SwSt 1, and fluorescence excitation by stellar continuum is concluded to be the dominant excitation mechanism. In this case, the alignment is bound to happen on the two excited levels $3P_{1,0}$ because of the anisotropy of the pumping radiation field, resulting polarizations in the [O I] $63, 145\mu m$ lines.

The high spatial resolution of SOFIA, for instance, is advantageous in zooming into PDRs and resolving the lines. Moreover, in highly turbulent environment, we expect that the magnetic field is entangled. The higher resolution means less averaging in the signals from atoms aligned with the magnetic field. The high sensitivity of the upgraded HAWC++ also provides us a possibility of doing precise quantitative measurement of the spectral polarizations, which can resolve the ambiguity of the 90 degree degeneracy and enables a 3D topology of magnetic field, which cannot be obtained from any other present magnetic diagnostics.

5.2 Metal detection in early universe

For instance, the distortion of CMB due to the optical pumping calculated accounting for the anisotropy of the optical/UV radiation field for the optically thin case differs from the result without anisotropy included [21]:

$$\begin{aligned}
y = \frac{\Delta I_\nu}{B_\nu(T_{CMB})} &= \tau \left\{ \frac{\tilde{\epsilon}_1 [\exp(T_*/T_{CMB}) - 1]}{\tilde{\eta} \exp(T_*/T_s) - \tilde{\eta}_s} - 1 \right\} \\
&= \tau_0 \left[\frac{\tilde{\epsilon}_1 [\exp(T_*/T_{CMB}) - 1]}{\exp(T_*/T_s) - 1} - \tilde{\tau} \right] \\
&\simeq \tau_0 [\tilde{\epsilon}_1 (1 + y_{iso}/\tau_0) - \tilde{\tau}] \\
&= \tilde{\epsilon}_1 y_{iso} + \tau_0 \frac{[w_{10}\sigma_0^2(J_l) - w_{0l}\sigma_0^2(J_l^0)](1 - 1.5 \sin^2 \theta)/\sqrt{2}}{1 - \exp(-T_*/T_s)} \quad (22)
\end{aligned}$$

where y_{iso} is the distortion neglecting the anisotropy of the radiation field and GSA (see [51]). Indeed if alignment is not accounted, then

$$y = y_{iso} = \tau_0 \frac{T_*}{T_s} \frac{\Delta T}{T_{cmb}} = \tau_0 \frac{T_{cmb}}{T_s} \exp\left(\frac{T_*}{T_{cmb}}\right) \left[1 - \frac{A(J_l^0)}{\sum_{J_l} A(J_l)} \right] \frac{[J_l^0] \beta B_m I_m}{[J_l] (A_m + B_m^s I_m)}, \quad (23)$$

where A_m, B_m, B_m^s are the Einstein coefficients for the magnetic dipole transitions within the ground state, and I_m is the corresponding line intensity, $\beta \equiv B I_\nu / B_m I_m$. Both $\tilde{\eta}_s$ and $\tilde{\tau}$ depend on the line of sight and the GSA (Eqs.19, 21), the resulting distortion in radiation is thus determined by the angle θ as well as the UV intensity of the OI line I_ν (or β , see Fig.9). Since both of the two terms on the right hand side of Eq.22 are proportional to β , the resulting distortion y is also proportional to β .

In some sense, this study is made for the case of weak pumping regimes discussed in [18]. But we take into account in addition the absorption and stimulated emission within the ground state.

5.3 Magnetic field in the epoch of reionization?

The issue of magnetic field at the epoch of reionization is a subject of controversies. The fact that the levels of O I ground state can be aligned through anisotropic pumping suggest us a possibility of using GSA to diagnose whether magnetic field exists at that early epoch.

The degree of polarization in the optically thin case can be obtained in a similar way as above by replacing $\tilde{\eta}_0, \tilde{\epsilon}_0$ by $\tilde{\eta}_1, \tilde{\epsilon}_1$. In the alignment regime, the

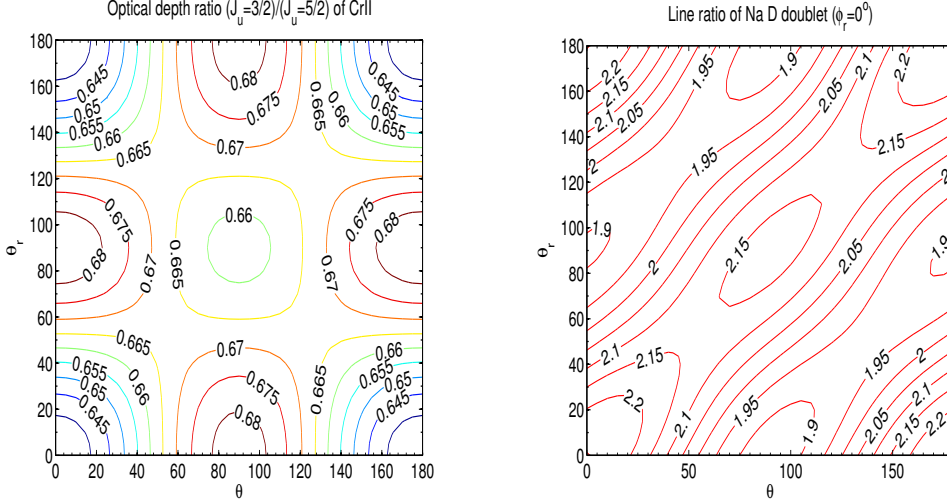


Fig. 10. *Left*: line ratio of Cr II absorption from the ground state to upper states $z6P_{3/2,5/2}^o$ (from [18]); *Right*: Contour graphs of the emissivity ratio of Na D doublet, ϕ_r is the azimuthal angle of the radiation in the reference frame where magnetic field defines the z axis and line of sight is in -x direction (from [19]).

7 Broad view of radiative alignment processes in Astrophysics

7.1 Ground state alignment

The alignment that we appeal to in the text above is related to the long-lived sublevels of the ground or metastable state. It is this effect that makes the alignment so sensitive to weak magnetic fields. Indeed, for the alignment to be sensitive to magnetic field, the life time of the sublevel should be longer than the Larmor precession time of an atom. This opens prospect of studying magnetic fields with intensities less than 10^{-7} G, covering the interesting range of magnetic field intensities in the ISM, intercluster medium and opening prospects of exploring magnetic fields in the intergalactic space and early Universe.

The use of the long-lived levels rather than excited levels, as for Hanle effect, allows studies of weak magnetic fields. The two effects can be used together, as it was discussed in [20].

7.2 Goldreich-Kylafis effect

There is another effect that has similarities to GSA. It is linear polarization in rotational molecular lines proposed first by [54, 55]. This effect also arises from uneven population of different sublevels, caused by anisotropy of radiation and

the resulting gradient in line optical depths. Since the rotational level is long lived, the sublevel population is also subjected to mixing by weak magnetic field. The linear polarization is also either perpendicular or parallel to the magnetic field; the degree of polarization depends on the angle between the line of sight, the symmetry axis of the radiation field, and the magnetic field.

Unlike GSA, the Goldreich-Kylafis effect arises from the pumping by the radiation between the same levels, rather than optical pumping. This makes the pumping dependent on the rather complex processes of radiation transfer and predicting of whether alignment and therefore the direction of polarization either parallel or perpendicular to magnetic field is rather difficult. In contrast, for the optical/UV pumping of GSA it should be possible frequently to identify the source of pumping radiation and therefore remove the ambiguity of the direction of polarization in respect to the magnetic field. An additional advantage arises from the possibility of a simultaneous use of many atomic species (both alignable and not alignable) in order to separate the physical and instrumental polarization. In addition, using several alignable species simultaneously, it is possible to get the 3D direction of magnetic field, which is impossible with the Goldreich-Kylafis effect.

7.3 Alignment processes in the solar atmosphere

A different regime of atomic alignment happens in strong magnetic field of solar atmosphere. Since the magnetic realignment requires that the magnetic mixing rate is larger than the optical pumping rate, it also happens in strong magnetic field regime if the radiation intensity is higher. The recent so-called “Second Solar Spectrum” ([29]; [56]) was rich in discussions of new atomic scattering processes. There are several anomalous polarimetric features in the profiles of the NaI D1 and D2 lines ([28]), the CaII IR triplet lines [57], and the MgI b1, b2, and b4 lines [58] that can only be understood in the context of atomic alignment. Solar polarimetrists now recognize that ground level atomic alignment has a significant, even dominant, influence for some lines [30]. There have been calls for a space-based mission to study the solar polarization with more lines.

As magnetic field strength decreases with the height, the detection of the Hanle and Zeeman effects gets more challenging. Upper chromosphere is the domain where GSA can provide unique opportunities for measuring magnetic field directions and its dynamics.

7.4 Grain alignment: comparison with GSA

Aligned grains provide a good way of tracing magnetic field. However, it has its limitations. We believe that techniques based on atomic and grain alignment processes are complementary.

Observationally it is known that grains tend to get aligned with long axes perpendicular to magnetic fields. The theory of grain alignment has long history (see [59] for a history of the subject overview). The current understanding is that grain alignment happens due to radiative torques¹⁰ (RATs) (see [9] for a review). We note that the RAT alignment of dust and GSA is similar: both processes depend on the action of anisotropic radiation.

The modern theory of grain alignment successfully explains the existing observational data. It predicts high efficiency of alignment in diffuse media with the efficiency decreasing for the high density molecular cores where grains are shielded from light. Unlike GSA, RATs align grains in a way that does not depend on the direction of the light anisotropy and the magnetic field (see [62]). Therefore there is no 90 degree ambiguity in polarization from dust, i.e. the polarization arising from dust seen in absorption is always parallel to magnetic field and the polarization of emission of dust is perpendicular to magnetic field. However, grains, unlike atoms, have individual and unknown shape which affects both the RATs and the efficiency of producing polarization. This is a deficiency of grain alignment compared to the GSA. This opens synergetic ways of using atomic and grain alignments as we discuss below.

It is important to note that RATs align only relatively large grains, i.e. for typical conditions in diffuse interstellar media grains larger than 5×10^{-6} cm are getting aligned (see [62]; [65]). Thus not all the extinction and emission is coming from aligned dust grains.

The grain alignment and GSA both have their own advantages and limitations. Atomic alignment has the ambiguity of 90 degree unless there is precise measurement of the degree of polarization. In the mean time, grains aligned by RAT does not depend on the direction of the light anisotropy and the magnetic field. Therefore there is no 90 degree ambiguity in polarization from dust. However, grains, unlike atoms, have individual and unknown shape which effects both RATs and the efficiency of producing polarization. This is a deficiency

¹⁰ RATs were first introduced in [60], but the results they obtained were inconclusive. The first numerical treatment of RATs which demonstrated the high efficiency was done in [61]. The analytical theory of RATs was presented in [62]. Further developments of the RAT theory, which include the effects of superparamagnetic inclusions in dust grains and the simultaneous action of RAT and other torques can be found in [63] and [64] respectively.

of grain alignment compared to the GSA.

The two techniques can complement each other. For instance, measurements of grain alignment in the region where GSA is mapped for a single species can remove the ambiguities in the magnetic field direction. At the same time, GSA is capable to produce a much more detailed map of magnetic field in the diffuse gas and measure magnetic field direction in the regions where the density of dust is insufficient to make any reliable measurement of dust polarization. The possibility of identifying regions of GSA for different species (e.g. ions can exist around strong ionization sources and the conditions for the alignment for different atoms/ions can be satisfied only in particular regions along the line of sight).

In addition, for interplanetary magnetic field measurements it is important that atomic alignment can measure magnetic fields on time scales much shorter than aligned grains are capable of. For the latter, the minimal time scale that they can trace should be larger than their Larmor period. For transient alignment, e.g. the alignment that takes place in the comet atmospheres (see [9]) the alignment time can also be a limitation in terms of tracing magnetic fields.

The advantage of techniques of grain alignment is that it is a well established observational technique. It can definitely help to test the new technique of GSA that we are discussing in this review.

7.5 *Studying magnetic field intensities*

Atomic alignment is usually by itself not directly sensitive to the magnetic field strength. The exception from this rule is a special case of pumping photon absorption rate being comparable with the Larmor frequency (see [20]). However, this should not preclude the use of GSA for studies of magnetic field.

Grain alignment according to the existing quantitative theory (see [62]) is not sensitive to magnetic field either. This does not prevent polarization arising from aligned grains to be used to study magnetic field strength with the so-called Chandrasekhar-Fermi technique [66]. In this technique the fluctuations of the magnetic field direction are associated with Alfvén perturbations¹¹ and therefore simultaneously measuring the velocity dispersion using optical/absorption lines arising from the same regions it is possible to estimate

¹¹ This is not a far fetched assumption, e.g. [67, 68] and [69] demonstrated the possibility of decomposing simulated MHD turbulence into Alfvén, slow and fast modes. Alfvén modes are known to be mostly responsible for magnetic field fluctuations and wandering ([70, 71]).

the magnetic field strength. The Chandrasekhar-Fermi technique and its modifications (see also [8], [72] for the modifications of the Chandrasekhar-Fermi technique) can be used to find magnetic field strength using GSA.

The advantage of using spectral lines compared to dust grains is that both polarization and line broadening can be measured from the same lines, making sure that both polarization and line broadening arise from the same volumes. In addition, GSA, unlike grain alignment does not contain ambiguities related to dust grain shape. Thus, potentially, Chandrasekhar-Fermi technique can be more accurate when GSA is used.

8 Prospects of studying magnetic field with aligned atoms

In this section, we illustrate the observational perspective by discussing a few synthetic observations with the input data on magnetic field from spacecraft measurements. We are fortunate to have in situ measurements of magnetic field in the interplanetary medium. The advantage of direct studies of magnetic perturbations by spacecrafts has been explored through many important missions. Such studies, unlike numerical ones, may deliver information about the actual magnetic turbulence at high Re and Rm numbers, where Re and Rm are the Reynolds and magnetic Reynolds number, respectively. However, the spacecraft measurement are rather expensive. Are there any other cost-effective ways to study magnetic turbulence in interplanetary medium?

Comets are known to have sodium tails and sodium is an atom that can be aligned by radiation and realigned by solar wind magnetic fields. This opens an opportunity of studying magnetic fields in the solar wind from the ground, by tracing the polarization of the Sodium line. At the moment this is a suggestion supported by the synthetic ground based observations. We conduct the synthetic observations for comets. For comets, we use a space weather model of magnetic field in [73] as well as the data collected by Vega1&2 during the encounter with comet Halley in 1986. The space weather model was developed by University of Michigan, namely, The Space Weather Modeling Framework (SWMG) [74]. More specifically, this is a solar corona and inner heliosphere model that extends the description of media from the solar surface to 1AU.

The structure of the magnetic field in the heliosphere can be studied by the polarization of Sodium D2 emission in the comet's wake. Though the abundance of sodium in comets is very low, its high efficiency in scattering sunlight makes it a good tracer [75]. As discussed in [19], the gaseous sodium atoms in the comet's tail acquire angular momentum from the solar radiation, i.e. they are aligned. Resonant scattering from these aligned atoms is polarized.

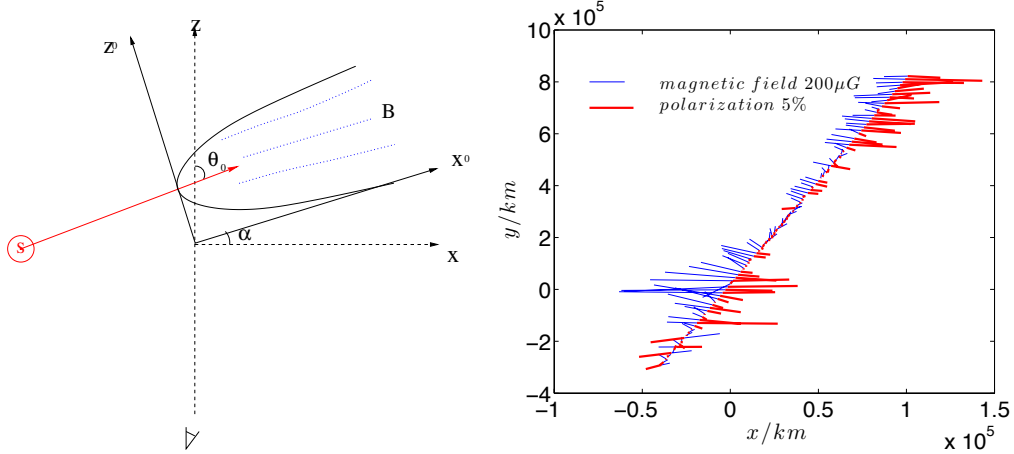


Fig. 11. *Left*: Schematics of the resonance scattering of sunlight by the sodium in comet wake. The sodium tail points in the direction opposite to the Sun. The observer on the Earth sees the stream at the angle θ_0 . Magnetic field realigns atoms via fast Larmor precession. Thus the polarization traces the interplanetary magnetic fields. *Right*: the magnetic field and polarization along the trajectory of Vega1 encountering the comet Halley (from [76]).

Distant from comets, the Sun can be considered a point source. As shown in Fig. 11, the geometry of the scattering is well defined, i.e., the scattering angle θ_0 is known. The alignment is modulated by the local magnetic field. The polarization of the sodium emission thus provides exclusive information on the magnetic field in the interplanetary medium. We take the data cube from the spacecraft measurement as described above. Depending on its direction, the embedded magnetic field alters the degree of alignment and therefore the polarization of the light scattered by the aligned atoms. Fig.11 illustrates the trajectory of a comet along which the magnetic field varies and the polarization of Sodium D2 emission changes accordingly. By comparing observations with them, we can cross-check our model and determine the structure of magnetic field in the heliosphere with similar observations. One can investigate not only spatial, but also *temporal* variations of magnetic fields. Since alignment happens at a time scale τ_R , magnetic field variations on this time scale will be reflected. This can allow for a cost-effective way of studying interplanetary magnetic turbulence at different scales.

On the basis of the results above we expect that comets may become an important source of information about interplanetary magnetic fields and their variations.

8.1 Synergy of techniques for magnetic field studies: role of atomic realignment

Above we mentioned the synergy of combining studies using atomic realignment and grain alignment. However, the synergy exists with other techniques as well. For instance, the atomic realignment, as we discussed above, allows to reveal the 3D direction of magnetic field. This gives the direction of the magnetic field, but not its amplitude. If Zeeman measurements allow to get the amplitude of the line of sight component magnetic field, this limited input enables atomic realignment to determine the entire 3D vector of magnetic field, including its amplitude. The importance of such synergetic measurements is difficult to overestimate.

As astrophysical magnetic fields cover a large range of scales, it is important to have techniques to study magnetic fields at different scales. In this respect atomic realignment fits a unique niche as it reveals small scale structure of magnetic field. For instance, we have discussed the possibility of studying magnetic fields in interplanetary medium. This can be done without conventional expensive probes by studying polarization of spectral lines. In some cases spreading of small amounts of sodium or other alignable species can produce detailed magnetic field maps of a particular regions of interplanetary space, e.g. the Earth magnetosphere.

9 Summary

Atomic realignment is an important effect the potential of which for magnetic field studies has not been yet tapped by the astrophysical community. The alignment itself is an effect studied well in the laboratory; the effects arise due to the ability of atoms/ions with fine and hyperfine structure to get aligned in the ground/metastable states. Due to the long life of the atoms in such states the Larmor precession in the external magnetic field imprints the direction of the field into the polarization of emitting and absorbing species. This provides a unique tool for studies of magnetic fields using polarimetry of UV, optical and radio lines. The range of objects for studies is extremely wide and includes magnetic fields in the early universe, in the interplanetary medium, in the interstellar medium, in circumstellar regions. Apart from this, the consequences of alignment should be taken into account for correct determining the abundances of alignable species.

Acknowledgments. We thank Ken Nordsieck for many insightful discussions about the practical procedures of measuring the GSA which substantially influenced our review. HY acknowledges the support from 985 grant from

Peking University and NSFC grant AST -11073004. AL's research is supported by the NSF AST 1109295 and the NSF Center for Magnetic Self-Organization (CMSO). He also acknowledges the Humboldt Award and related productive stay at the Universities of Bohum and Cologne as well as a visiting fellowship at the International Institute of Physics (Brazil).

A Irreducible density matrix

We adopt the irreducible tensorial formalism for performing the calculations (see also YL04). The relation between irreducible tensor and the standard density matrix of atoms is

$$\rho_Q^K(F, F') = \sum_{MM'} (-1)^{F-M} (2K+1)^{1/2} \begin{pmatrix} F & K & F' \\ -M & Q & M' \end{pmatrix} \langle FM|\rho|F'M' \rangle. \quad (\text{A.1})$$

For photons, their generic expression of irreducible spherical tensor is:

$$J_Q^K = \sum_{qq'} (-1)^{1+q} [3(2K+1)]^{1/2} \begin{pmatrix} 1 & 1 & K \\ q & -q' & -Q \end{pmatrix} J_{qq'}, \quad (\text{A.2})$$

References

- [1] R. M. Crutcher, N. Hakobian, T. H. Troland, Self-consistent analysis of OH Zeeman observations, *MNRAS* 402 (2010) L64–L66.
- [2] R. M. Crutcher, T. H. Troland, Testing Faraday Rotation Estimates of Magnetic Field Strengths toward Dark Clouds, *ApJ* 685 (2008) 281–284.
- [3] R. Beck, Cosmic Magnetic Fields: Observations and Prospects, in: F. A. Aharonian, W. Hofmann, & F. M. Rieger (Ed.), *American Institute of Physics Conference Series*, volume 1381 of *American Institute of Physics Conference Series*, pp. 117–136.
- [4] A. Lazarian, D. Pogosyan, A. Esquivel, Quest for H I Turbulence Statistics: New Techniques, in: A. R. Taylor, T. L. Landecker, & A. G. Willis (Ed.), *Seeing Through the Dust: The Detection of HI and the Exploration of the ISM in Galaxies*, volume 276 of *Astronomical Society of the Pacific Conference Series*, p. 182.
- [5] A. Esquivel, A. Lazarian, Velocity Centroids as Tracers of the Turbulent Velocity Statistics, *ApJ* 631 (2005) 320–350.
- [6] A. Esquivel, A. Lazarian, Velocity Anisotropy as a Diagnostic of the Magnetization of the Interstellar Medium and Molecular Clouds, *ApJ* 740 (2011) 117.

- [7] A. Lazarian, D. Pogosyan, Statistical Description of Synchrotron Intensity Fluctuations: Studies of Astrophysical Magnetic Turbulence, *ApJ* 747 (2012) 5.
- [8] R. H. Hildebrand, Magnetic Fields in Molecular Clouds, in: D. C. Lis, J. E. Vaillancourt, P. F. Goldsmith, T. A. Bell, N. Z. Scoville, & J. Zmuidzinas (Ed.), *Submillimeter Astrophysics and Technology: a Symposium Honoring Thomas G. Phillips*, volume 417 of *Astronomical Society of the Pacific Conference Series*, p. 257.
- [9] A. Lazarian, Tracing magnetic fields with aligned grains, *Journal of Quantitative Spectroscopy and Radiative Transfer* 106 (2007) 225–256.
- [10] E. Landi Degl’Innocenti, M. Landolfi (Eds.), *Polarization in Spectral Lines*, volume 307 of *Astrophysics and Space Science Library*, 2004.
- [11] A. Kastler, Quelques suggestions concernant la production optique et la détection optique d’une inégalité de population des niveaux de quantification spatiale des atomes. Application à l’expérience de Stern et Gerlach et à la résonance magnétique, *J. Phys. Radium* 11 (1950) 255–265.
- [12] Brossel, Jean, Kastler, Alfred, Winter, Jacques, Création optique d’une inégalité de population entre les sous-niveaux zeeman de l’état fondamental des atomes, *J. Phys. Radium* 13 (1952) 668.
- [13] W. B. Hawkins, R. H. Dicke, The polarization of sodium atoms, *Phys. Rev.* 91 (1953) 1008–1009.
- [14] W. B. Hawkins, Orientation and Alignment of Sodium Atoms by Means of Polarized Resonance Radiation, *Physical Review* 98 (1955) 478–486.
- [15] C. Cohen-Tannoudji, J. Dupont-Roc, S. Haroche, F. Laloë, Detection of the Static Magnetic Field Produced by the Oriented Nuclei of Optically Pumped ^3He Gas, *Physical Review Letters* 22 (1969) 758–760.
- [16] D. A. Varshalovich, Reviews of Topical Problems: Spin States of Atoms and Molecules in the Cosmic Medium, *Soviet Physics Uspekhi* 13 (1971) 429–437.
- [17] M. Landolfi, E. Landi Degl’Innocenti, Resonance scattering and the diagnostic of very weak magnetic fields in diffuse media, *A&A* 167 (1986) 200–206.
- [18] H. Yan, A. Lazarian, Polarization of Absorption Lines as a Diagnostics of Circumstellar, Interstellar, and Intergalactic Magnetic Fields: Fine-Structure Atoms, *ApJ* 653 (2006) 1292–1313.
- [19] H. Yan, A. Lazarian, Polarization from Aligned Atoms as a Diagnostic of Circumstellar, Active Galactic Nuclei, and Interstellar Magnetic Fields. II. Atoms with Hyperfine Structure, *ApJ* 657 (2007) 618–640.
- [20] H. Yan, A. Lazarian, Atomic Alignment and Diagnostics of Magnetic Fields in Diffuse Media, *ApJ* 677 (2008) 1401–1424.
- [21] H. Yan, A. Lazarian, Ground-state alignment of atoms and ions: New Diagnostics of Astrophysical Magnetic Field in Diffuse Medium, in: *Revista Mexicana de Astronomia y Astrofisica Conference Series*, volume 36 of *Revista Mexicana de Astronomia y Astrofisica Conference Series*, pp. 97–105.

- [22] W. Happer, Optical Pumping, *Reviews of Modern Physics* 44 (1972) 169–249.
- [23] D. Budker, M. Romalis, Optical magnetometry, *Nature Physics* 3 (2007) 227–234.
- [24] D. A. Varshalovich, The dynamic orientation of particle spins in space., *Astrofizika* 4 (1968) 519–536.
- [25] D. A. Varshalovich, G. F. Chorny, Determination of magnetic field direction in a comet’s head, *Icarus* 43 (1980) 385–390.
- [26] E. Landi Degl’Innocenti, Polarization in spectral lines. I - A unifying theoretical approach., *Solar Phys.* 85 (1983) 3–31.
- [27] E. Landi Degl’Innocenti, Polarization in spectral lines. III - Resonance polarization in the non-magnetic, collisionless regime, *Solar Phys.* 91 (1984) 1–26.
- [28] E. Landi Degl’Innocenti, Evidence against turbulent and canopy-like magnetic fields in the solar chromosphere, *Nat* 392 (1998) 256.
- [29] J. O. Stenflo, C. U. Keller, The second solar spectrum. A new window for diagnostics of the Sun., *A&A* 321 (1997) 927–934.
- [30] J. Trujillo Bueno, E. Landi Degl’Innocenti, Linear Polarization due to Lower Level Depopulation Pumping in Stellar Atmospheres, *ApJ* 482 (1997) L183.
- [31] J. Trujillo Bueno, E. Landi Degl’Innocenti, M. Collados, L. Merenda, R. Manso Sainz, Selective absorption processes as the origin of puzzling spectral line polarization from the Sun, *Nat* 415 (2002) 403–406.
- [32] K. Nordsieck, R. Ignace, The Hanle Effect in P Cygni Wind Lines, in: A. Adamson, C. Aspin, C. Davis, & T. Fujiyoshi (Ed.), *Astronomical Polarimetry: Current Status and Future Directions*, volume 343 of *Astronomical Society of the Pacific Conference Series*, p. 284.
- [33] J. R. Kuhn, S. V. Berdyugina, D. M. Fluri, D. M. Harrington, J. O. Stenflo, A New Mechanism for Polarizing Light from Obscured Stars, *ApJ* 668 (2007) L63–L66.
- [34] K. Nordsieck, Atomic Fluorescence and Prospects for Observing Magnetic Geometry Using Atomic Magnetic Realignment, *ArXiv e-prints* (2008).
- [35] A. Kastler, Optical methods of atomic orientation and of magnetic resonance, *Journal of the Optical Society of America* (1917-1983) 47 (1957) 460.
- [36] D. C. Morton, Interstellar absorption lines in the spectrum of zeta Ophiuchi, *ApJ* 197 (1975) 85–115.
- [37] B. D. Savage, B. P. Wakker, A. J. Fox, K. R. Sembach, FUSE Observations of Interstellar and Intergalactic Absorption toward the X-Ray-bright BL Lacertae Object Markarian 421, *ApJ* 619 (2005) 863–883.
- [38] D. A. Verner, P. D. Barthel, D. Tytler, Atomic data for absorption lines from the ground level at wavelengths greater than 228Å., *Astronomy and Astrophysics Suppl.* 108 (1994) 287–340.
- [39] M. M. Litvak, A. L. McWhorter, M. L. Meeks, H. J. Zeiger, Maser Model for Interstellar OH Microwave Emission, *Physical Review Letters*

- 17 (1966) 821–826.
- [40] F. Perkins, T. Gold, E. E. Salpeter, Maser Action in Interstellar OH, *ApJ* 145 (1966) 361.
- [41] F. H. Mies, Ultraviolet Fluorescent Pumping of OH 18-CENTIMETER Radiation in Comets, *ApJ* 191 (1974) L145.
- [42] E. Rausch, W. H. Kegel, T. Tsuji, G. Piehler, Optical pumping of circumstellar SiO masers., *A&A* 315 (1996) 533–541.
- [43] N. P. Abel, G. J. Ferland, C. R. O’Dell, G. Shaw, T. H. Troland, Physical Conditions in Orion’s Veil. II. A Multicomponent Study of the Line of Sight toward the Trapezium, *ApJ* 644 (2006) 344–354.
- [44] A. C. Carciofi, J. E. Bjorkman, K. S. Bjorkman, Modeling the Circumstellar Disk of ζ Tauri, in: A. Adamson, C. Aspin, C. Davis, & T. Fujiyoshi (Ed.), *Astronomical Polarimetry: Current Status and Future Directions*, volume 343 of *Astronomical Society of the Pacific Conference Series*, p. 417.
- [45] S. A. Grandi, Starlight excitation of permitted lines in the Orion Nebula, *ApJ* 196 (1975) 465–472.
- [46] S. A. Grandi, Observations of Starlight-Excited Lines in the Orion Nebula, *ApJ* 199 (1975) L43.
- [47] B. Sharpee, J. A. Baldwin, R. Williams, Identification and Characterization of Faint Emission Lines in the Spectrum of the Planetary Nebula IC 418, *ApJ* 615 (2004) 323–343.
- [48] S. A. Wouthuysen, On the excitation mechanism of the 21-cm (radio-frequency) interstellar hydrogen emission line., *AJ* 57 (1952) 31–32.
- [49] G. Field, Excitation of the hydrogen 21-cm line, *Proceedings of the IRE* 46 (1958) 240–250.
- [50] S. R. Furlanetto, S. P. Oh, F. H. Briggs, Cosmology at low frequencies: The 21 cm transition and the high-redshift Universe, *PhysRep* 433 (2006) 181–301.
- [51] C. Hernández-Monteagudo, J. A. Rubiño-Martín, R. A. Sunyaev, On the influence of resonant scattering on cosmic microwave background polarization anisotropies, *MNRAS* 380 (2007) 1656–1668.
- [52] J. Lequeux, *The Interstellar Medium*, 2005.
- [53] N. C. Sterling, H. L. Dinerstein, C. W. Bowers, S. Redfield, The FUSE Spectrum of the Planetary Nebula SwSt 1: Evidence for Inhomogeneities in the Gas and Dust, *ApJ* 625 (2005) 368–384.
- [54] P. Goldreich, N. D. Kylafis, On mapping the magnetic field direction in molecular clouds by polarization measurements, *ApJ* 243 (1981) L75–L78.
- [55] P. Goldreich, N. D. Kylafis, Linear polarization of radio frequency lines in molecular clouds and circumstellar envelopes, *ApJ* 253 (1982) 606–621.
- [56] A. M. Gandorfer, A High Resolution Atlas of the Second Solar Spectrum, in: M. Sigwarth (Ed.), *Advanced Solar Polarimetry – Theory, Observation, and Instrumentation*, volume 236 of *Astronomical Society of the Pacific Conference Series*, p. 109.
- [57] R. Manso Sainz, J. Trujillo Bueno, Modeling the Scattering Line Polar-

- ization of the Ca II Infrared Triplet, in: M. Sigwarth (Ed.), *Advanced Solar Polarimetry – Theory, Observation, and Instrumentation*, volume 236 of *Astronomical Society of the Pacific Conference Series*, p. 213.
- [58] J. Trujillo Bueno, Atomic Polarization and the Hanle Effect, in: M. Sigwarth (Ed.), *Advanced Solar Polarimetry – Theory, Observation, and Instrumentation*, volume 236 of *Astronomical Society of the Pacific Conference Series*, p. 161.
- [59] A. Lazarian, Magnetic Fields via Polarimetry: Progress of Grain Alignment Theory, *Journal of Quantitative Spectroscopy and Radiative Transfer* 79 (2003) 881–902.
- [60] A. Z. Dolginov, I. G. Mitrofanov, Orientation of cosmic dust grains, *Astrophysics and Space Science* 43 (1976) 291–317.
- [61] B. T. Draine, J. C. Weingartner, Radiative Torques on Interstellar Grains. I. Superthermal Spin-up, *ApJ* 470 (1996) 551.
- [62] A. Lazarian, T. Hoang, Radiative torques: analytical model and basic properties, *MNRAS* 378 (2007) 910–946.
- [63] A. Lazarian, T. Hoang, Alignment of Dust with Magnetic Inclusions: Radiative Torques and Superparamagnetic Barnett and Nuclear Relaxation, *ApJ* 676 (2008) L25–L28.
- [64] T. Hoang, A. Lazarian, Radiative Torques Alignment in the Presence of Pinwheel Torques, *ApJ* 695 (2009) 1457–1476.
- [65] T. Hoang, A. Lazarian, Radiative torque alignment: essential physical processes, *MNRAS* 388 (2008) 117–143.
- [66] S. Chandrasekhar, E. Fermi, Magnetic Fields in Spiral Arms., *ApJ* 118 (1953) 113.
- [67] J. Cho, A. Lazarian, Compressible Sub-Alfvénic MHD Turbulence in Low- β Plasmas, *Physical Review Letters* 88 (2002) 245001–+.
- [68] J. Cho, A. Lazarian, Compressible magnetohydrodynamic turbulence: mode coupling, scaling relations, anisotropy, viscosity-damped regime and astrophysical implications, *MNRAS* 345 (2003) 325–339.
- [69] G. Kowal, A. Lazarian, Velocity Field of Compressible Magnetohydrodynamic Turbulence: Wavelet Decomposition and Mode Scalings, *ApJ* 720 (2010) 742–756.
- [70] A. Lazarian, E. T. Vishniac, Reconnection in a Weakly Stochastic Field, *ApJ* 517 (1999) 700–718.
- [71] A. Lazarian, E. T. Vishniac, J. Cho, Magnetic Field Structure and Stochastic Reconnection in a Partially Ionized Gas, *ApJ* 603 (2004) 180–197.
- [72] D. Falceta-Gonçalves, A. Lazarian, G. Kowal, Studies of Regular and Random Magnetic Fields in the ISM: Statistics of Polarization Vectors and the Chandrasekhar-Fermi Technique, *ApJ* 679 (2008) 537–551.
- [73] Y. C.-M. Liu, M. Opher, O. Cohen, P. C. Liewer, T. I. Gombosi, A Simulation of a Coronal Mass Ejection Propagation and Shock Evolution in the Lower Solar Corona, *ApJ* 680 (2008) 757–763.
- [74] G. Tóth, I. V. Sokolov, T. I. Gombosi, D. R. Chesney, C. R. Clauer, D. L.

- De Zeeuw, K. C. Hansen, K. J. Kane, W. B. Manchester, R. C. Oehmke, K. G. Powell, A. J. Ridley, I. I. Roussev, Q. F. Stout, O. Volberg, R. A. Wolf, S. Sazykin, A. Chan, B. Yu, J. Kóta, Space Weather Modeling Framework: A new tool for the space science community, *Journal of Geophysical Research (Space Physics)* 110 (2005) 12226.
- [75] N. Thomas, Optical observations of Io's neutral clouds and plasma torus, *Surveys in Geophysics* 13 (1992) 91–164.
- [76] J. Shangguan, H. Yan, Study of Interplanetary Magnetic Field with Atomic Alignment, *ArXiv e-prints* (2010).